ORNL-TM-2952

Contract No. W-7403-eng-26

REACTOR DIVISION

PARAMETRIC SURVEY OF THE EFFECTS OF MAJOR PARAMETERS ON THE DESIGN OF FUEL-TO-INERT-SALT HEAT EXCHANGERS FOR THE MSBR

A. P. Fraas and M. E. LaVerne

NOVEMBER 1971

OAK RIDGE NATIONAL LABORATORY
Oak Ridge, Tennessee 37830
operated by
UNION CARBIDE CORPORATION
for the
U.S. ATOMIC ENERGY COMMISSION

CONTENTS

PARAMETRIC SURVEY OF THE EFFECTS OF MAJOR PARAMETERS ON THE DESIGN OF FUEL-TO-INERT-SALT HEAT EXCHANGERS FOR MOLTEN SALT REACTORS

A. P. Fraas and M. E. LaVerne

ABSTRACT

The design of heat exchangers for molten salt reactors involves so many parameters and their interrelationships are so complex that it is difficult to envision the effects of the various trade-offs that can be made in attempts to optimize the system. This report presents a procedure for carrying out such analyses together with the results of a parametric study showing the effects of tube diameter, fuel pressure drop, inert salt pressure drop, and the temperature difference between the fuel and the inert salt with either $NaBF_4$ or Flinak as the fluid in the intermediate heat transport system. An unusual design for a 2200 Mw(t), 100 Mw(e) power plant[1] was used as the reference design for the detailed calculations of the parametric study presented in this report.

INTRODUCTION

In response to a request from R. B. Briggs of this Laboratory, A. P. Fraas worked out a conceptual design for a molten-salt breeder reactor in which the heat exchangers and the pumps were enclosed with the reactor in a single pressure vessel.[1] This design approach was taken in part to minimize the fuel inventory in the system and in part to avoid difficulties with thermal stresses and possible thermal stress cracking that might be caused by differential expansion in connecting piping. Extremely difficult problems arise in piping systems in which the pipe length-diameter ratio is too low to give good flexibility for accommodation of the differential thermal expansion between the hot and cold portions of the system. This is particularly so because the system must also be designed to withstand a severe earthquake.

When the report describing the integrated reactor-heat exchanger design was circulated in rough draft form, quite a number of people raised questions with regard to the effects on fuel inventory of changes in the major design parameters. The analysis presented in the following section was therefore carried out to answer these questions. Inasmuch as the

calculational technique and computer program have general application, it seemed desirable to present the study in this report.

SUMMARY

An analysis has been made of the performance of fuel-to-inert-salt heat exchangers for the MSBR. Employing this analysis, a parametric study has been made of the effects on the heat exchanger design of changes in the input parameters of major interest. The result is to clarify the effects of the various trade-offs that can be made in attempts to optimize the system design. Table 1 is a concise summary of the principal results of the parametric study.

Table 1. Summary of Effects of Changes in Major Parameters on Number of Tubes, Tube Length, and Heat Exchanger Fuel Inventory

Parameter and Change	Approximate Percentage Effect		
	Number of Tubes	Tube Length	Fuel Inventory
Tube OD 3/8 to 5/16 in.	+40	-20	-25
Fuel Δp(Δp_s) 100 to 200 psi	- 5	-10	-30
Salt Δp(Δp_t) 100 to 200 psi	-25	+25	+20
Salt $NaBF_4$ to Flinak	-10	-10	-20
Temperature difference (ΔT)			
100 to 125°F	-10	-15	-25
100 to 150°F	-15	-30	-40

Minimization of the heat exchanger fuel inventory is highly desirable. As can be seen from Table 1, the fuel inventory can be reduced by decreasing the tube size, increasing the fuel pressure drop, changing the inert salt from $NaBF_4$ to Flinak, and by increasing the temperature difference between the fuel and inert salt. Note that, in contrast with the effect of the fuel pressure drop, the fuel inventory is increased by an increase

in the inert salt pressure drop. From the table, one can deduce that, if all the parameter changes producing reductions were employed, a reduction in heat exchanger fuel inventory of as much as 62% could be obtained over the reference design conditions. For the full-scale 1000 Mw(e) reactor system described in Ref. 1, this would mean a reduction in total system fuel inventory from approximately 1185 ft^3 to approximately 871 ft^3 for $NaBF_4$ and from about 1095 ft^3 to about 825 ft^3 for Flinak.

Fabrication costs for a tube bundle will depend primarily on the number of tubes in the bundle, because this determines the number of header welds required. Material costs will vary with tube length and the total tube cross-sectional area. For the same set of parameter changes employed above with respect to fuel inventory, one finds virtually no change in the number of tubes and, thus, essentially an unchanged fabrication cost. Tube length, from Table 1, is reduced by a factor of approximately 0.45. The smaller tube cross-sectional area contributes a further factor of 0.68, for an overall reduction factor of about 0.3, that is, a reduction in material weight of nearly 70%.

A substantial fraction of the above savings is predicated on the ability to increase the temperature difference between the fuel and inert salt from 100 to 150°F. Experience gained in the ANP Program with thermal stresses indicated that it is not difficult to assure a high degree of reliability and freedom from difficulties with thermal stresses if the temperature difference between the two fluid circuits does not exceed 100°F. However, with careful design it seems likely that the temperature difference might be increased to as much as 150°F without deleterious effects provided that both a thorough analysis and near full-scale tests could be carried out.

As can be shown from the equations in the analysis of this report for a given system and fluid temperature rise, the pumping power in either fluid circuit depends only on the salt properties and the pressure drop in that circuit, being linear in the pressure drop. Thus, for a given fuel and inert salt combination, the pumping power can be reduced only by reducing the pressure drop. For a given fuel and set of specified operating conditions, the pumping power can be reduced 10 to 20% by using Flinak in

place of $NaBF_4$ in the secondary circuit. The savings in total heat exchanger pumping power range from 10 to 20%, depending only on the ratio of the inert salt pressure drop to the fuel pressure drop.

ANALYSIS

The analysis presented in this section is predicated on the use of smooth, round tubes on an equilateral triangular pitch with axial fluid flow outside the tubes. Conventional, well-established relationships were used for the various heat balance, convective heat transfer, and pressure drop equations employed. (Recent experiments with molten salt favor reducing the heat transfer coefficients about 15% from the values used here.)

Design Bases and Criteria

The analysis and parametric study presented in this report were carried out on the basis of a U-tube heat exchanger tube bundle having the tubes in an equilateral triangular pattern with the fuel salt flowing axially on the shell side and the inert salt (in the secondary circuit) in counterflow on the tube side as described in Ref. 1. A cross section of the exchanger configuration envisaged is shown in Fig. 1. However, as will be seen subsequently, the analysis is by no means limited to the particular configuration and conditions treated here but is applicable to a much wider range of problems.

The tubes were placed on an equilateral triangular pitch, rather than a square pitch, in order to increase the thickness of the fluid stream in the region between adjacent tubes because data from ANP heat exchanger tests had indicated that thin fluid ligaments between tubes lead to flow stratification and a loss in heat transfer performance. This effect was deduced from the curves in Figs. 2 and 3, which were obtained with ANP heat exchangers.[2]

The tube spacers, consisting of "combs" of flattened wire, employed in the ANP heat exchangers could be used with the equilateral triangular spacing considered here. That approach would yield an increase in pressure drop by a factor of about 1.5 over that for the ideal case with no spacers. It seems likely that spiral wire spacers would lead to an

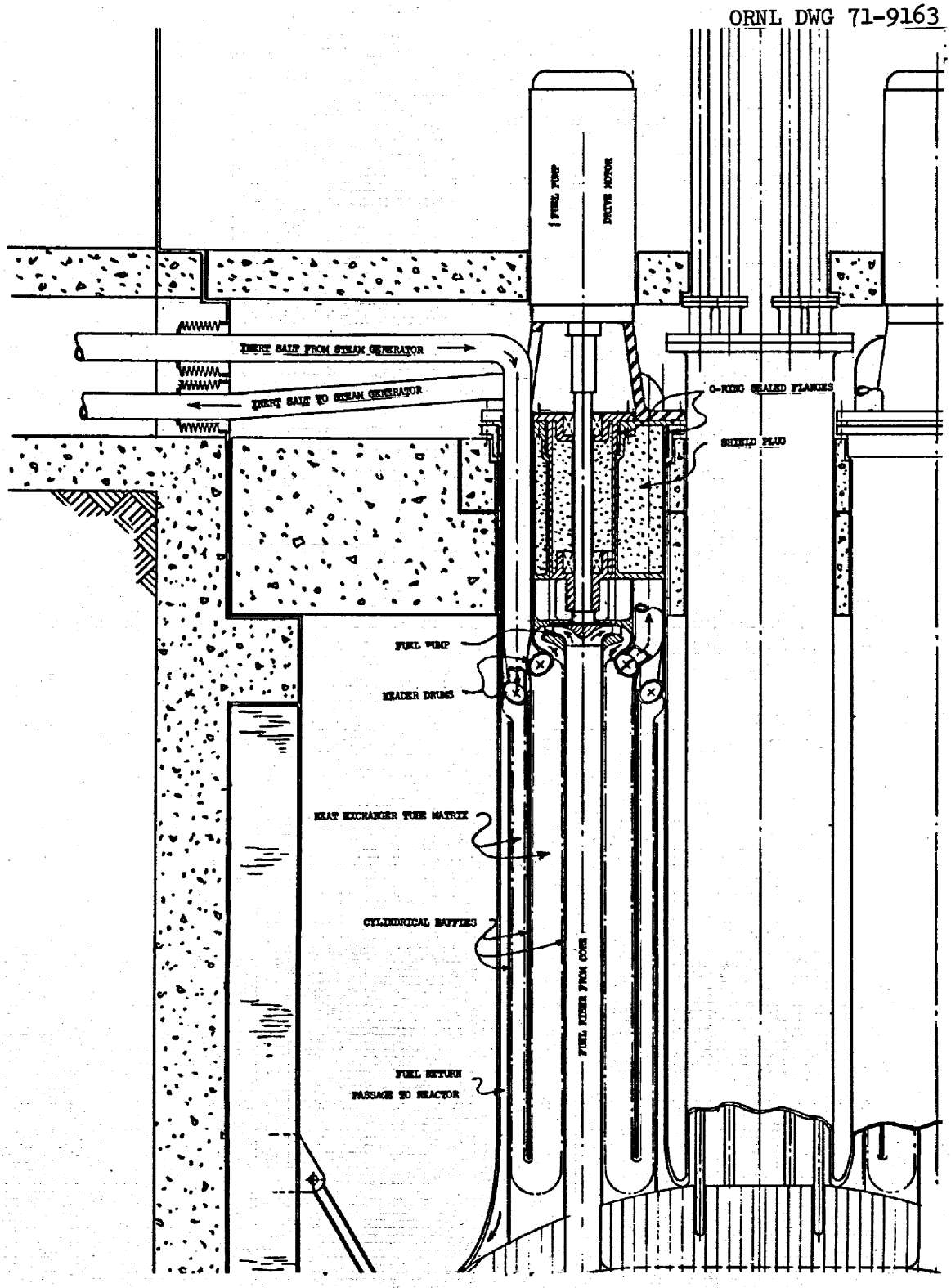

Fig. 1. Tube Bundle for One of the Six Fuel-to-Inert Salt Heat Exchangers Employed in Parallel in the Conceptual Design of Ref. 1 for a 2200 Mw(t) Reactor.

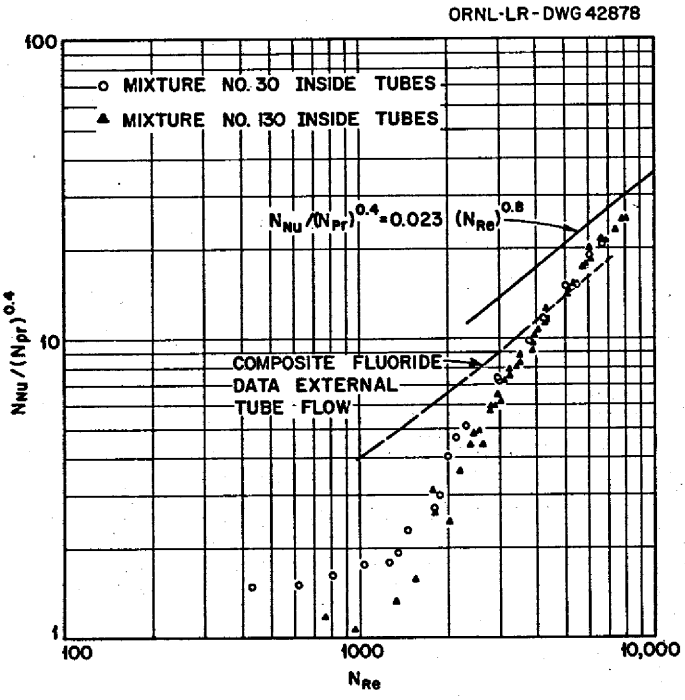

Fig. 2. The Heat-Transfer Characteristics of a Molten Salt When Flowing Inside Round Tubes (Yarosh, Ref. 2).

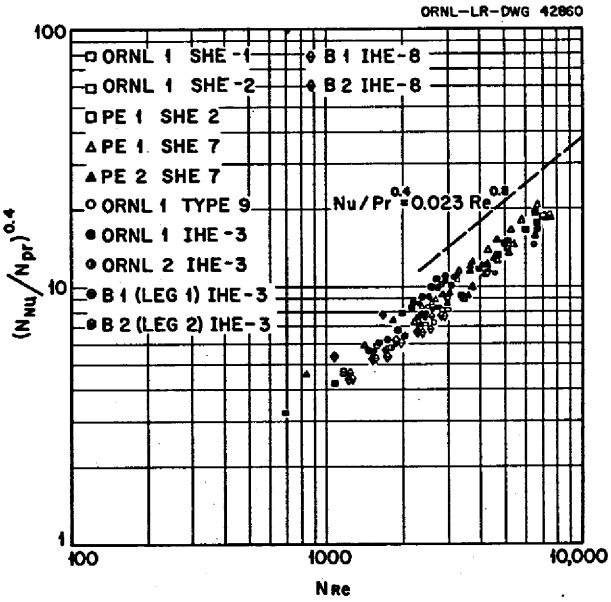

Fig. 3. The Heat-Transfer Characteristics of a Molten Salt Flowing on the Shell Side of Twelve Different Z-Tube Heat Exchangers Tested in Six Different Systems (Yarosh, Ref. 2).

increase in pressure drop somewhat less than this and they might also have a somewhat more favorable effect on the heat transfer coefficient, but no clear-cut data are available. A definitive answer to these questions would require testing of the exact geometry of the heat exchanger matrix contemplated.

Similarly, the effects of various types of surface roughness designed to increase the heat transfer coefficient, in fact, are very difficult to predict and will also require tests of the exact geometry contemplated in order to determine the extent to which the heat transfer coefficient is improved at the expense of an increase in pressure drop. Because it appears that surface roughness frequently has not paid important dividends for cases of the type of interest here, and because of the uncertainties involved, it was decided to conduct the analysis assuming bare, smooth tubes with no allowances for spacers. Inclusion of the latter would increase the fuel pressure drop by around 30 to 50%, but should also increase the heat transfer coefficient somewhat so that, with an equilateral triangular tube pattern, the shell-side heat transfer coefficient might well be higher than for the corresponding circular passages inside the round tubes.

Derivation of Heat Exchanger Equations

We assume that the heat exchanger tube bundle is composed of round, smooth tubes with axial fluid flow outside the tubes. We neglect entrance effects and the shell-side pressure drop associated with the tube spacers. Nomenclature for the analysis is given in Table 2.

Heat Balances

The axial heat transport is given in terms of the mass flows, fluid temperature changes, and exchanger geometry by

$$Q = G_s A_s C_{ps} \delta T_s \qquad (1)$$

and

Table 2. Nomenclature

Symbol	Meaning	Units
A	Axial flow area	ft^2
C_p	Specific heat	$Btu/lb_m \cdot F$
D	Diameter	ft
f	Blasius friction factor	
G	Mass velocity	$lb_m/hr \cdot ft^2$
g_c	Dimensional conversion constant	$lb_m ft/lb_f \cdot hr^2$ (4.170×10^8)
h	Heat transfer coefficient	$Btu/hr \cdot ft^2 \cdot F$
k	Thermal conductivity	$Btu/hr \cdot ft \cdot F$
L	Tube length	ft
N	Number of tubes	
ΔP	Pressure difference	lb_f/ft^2
Q	Heat transfer rate	Btu/hr
$S_1 - S_5$	Shell-side coefficients and exponents	
$T_1 - T_5$	Tube-side coefficients and exponents	
ΔT	Film temperature difference	F degrees
δT	Fluid axial temperature difference	F degrees
t	Thickness	ft
μ	Viscosity	$lb_m/hr \cdot ft$
ρ	Density	lb_m/ft^3
Subscripts		
m	Mean	
o	Outside	
s	Shell side	
t	Tube side	
w	Tube wall	

$$Q = G_t \frac{\pi}{4} D_t^2 N C_{pt} \delta T_t \ . \tag{2}$$

The radial heat transport by convection and conduction through the two fluid films and the tube wall, respectively, is given by

$$Q = h_s \pi D_o L N \Delta T_s \ , \tag{3}$$

$$Q = h_t \pi D_t L N \Delta T_t \ , \tag{4}$$

and

$$Q = k_w \pi D_m L N \Delta T_w / t_w \ . \tag{5}$$

Convective Heat Transfer

The convective heat transfer relations employed here are those of Sieder and Tate[3] for laminar flow, and Colburn[4] for turbulent flow. Both relations may be expressed in the form given by Eqs. 6 and 7, where the several coefficients and exponents are determined from Table 3 according to the flow regime.

$$\frac{h_s D_s}{k_s} = S_1 \left(\frac{L}{D_s}\right)^{-S_2} \left(\frac{G_s D_s}{\mu_s}\right)^{S_3} \left(\frac{C_{ps} \mu_s}{k_s}\right)^{1/3} \tag{6}$$

$$\frac{h_t D_t}{k_t} = T_1 \left(\frac{L}{D_t}\right)^{-T_2} \left(\frac{G_t D_t}{\mu_t}\right)^{T_3} \left(\frac{C_{pt} \mu_t}{k_t}\right)^{1/3} \tag{7}$$

Temperature Difference Between Fluids

The overall temperature difference, ΔT, between the two fluids is given by the summation of the temperature differences through the two fluid films and the tube wall,

$$\Delta T = \Delta T_s + \Delta T_w + \Delta T_t \ . \tag{8}$$

Table 3. Coefficients and Exponents Used in Convective Heat Transfer and Friction Factor Equations

	S_1	S_2	S_3	S_4	S_5
Outside tubes (shell side)					
Laminar flow	$4/\sqrt[3]{10}$	1/3	1/3	64	1
Turbulent flow	0.032	0	4/5	0.256	1/5
	T_1	T_2	T_3	T_4	T_5
Inside tubes (tube side)					
Laminar flow	$4/\sqrt[3]{10}$	1/3	1/3	64	1
Turbulent flow	0.023	0	4/5	0.184	1/5

Note: The coefficient S_1 for turbulent flow is obtained from Ref. 5.

Pressure Drops

The pressure drop on the shell side is given by the Blasius relation,

$$\Delta P_s = f_s \frac{L}{D_s} \frac{G_s^2}{2g_c \rho_s} , \tag{9a}$$

where the friction factor is defined, in terms of the shell-side Reynolds number, by

$$f_s = S_4 \left(\frac{G_s D_s}{\mu_s} \right)^{-S_5} . \tag{9b}$$

Similarly, the tube-side pressure drop is determined from

$$\Delta P_t = f_t \frac{L}{D_t} \frac{G_t^2}{2g_c \rho_t} \tag{10a}$$

and

$$f_t = T_4\left(\frac{G_t D_t}{\mu_t}\right)^{-T_5} \tag{10b}$$

The coefficients and exponents appearing in the expressions for the friction factors also are determined from Table 2 according to the flow regime.

Shell-Side Equivalent Diameter

The equivalent diameter of the shell-side flow passage is determined from the definition,

$$D_s = \frac{4A_s}{\pi D_o N} \tag{11}$$

Solution of the Equations

Let us take as input parameters (independent variables) the total heat transport, the pressure drops on the shell and tube-sides, the tube size, the temperature changes in the two fluid streams, and the overall temperature difference between the fluids. Then, the foregoing set of 11 equations is just sufficient to determine the two mass flows, the equivalent diameter and flow area on the shell side, the overall length and number of tubes in the bundle, the three transverse temperature differences, and the two heat transfer coefficients, 11 dependent variables in all.

Reduction to a Single Equation

Let us now eliminate the friction factors between Eqs. 9a and 9b and between Eqs. 10a and 10b. Rewriting the remaining equations with only known quantities on their right hand sides then yields

$$G_s A_s = C_1 = \frac{Q}{C_{ps}\delta T_s}, \tag{12}$$

$$G_t N = C_2 = \frac{Q}{\frac{\pi}{4} D_t^2 C_{pt} \delta T_t}, \tag{13}$$

$$h_s LN\Delta T_s = C_3 = \frac{Q}{\pi D_o} , \tag{14}$$

$$h_t LN\Delta T_t = C_4 = \frac{Q}{\pi D_t} , \tag{15}$$

$$LN\Delta T_w = C_5 = \frac{Qt_w}{\pi D_m k_w} , \tag{16}$$

$$h_s D_s^{1-S_2-S_3} L^{S_2} G_s^{-S_3} = C_6 = S_1 \left(C_{ps} k_s^2 \right)^{1/3} \mu_s^{1/3-S_3} , \tag{17}$$

$$h_t L^{T_2} G_t^{-T_3} = C_7 = T_1 \left(C_{pt} k_t^2 \right)^{1/3} \mu_t^{1/3-T_3} D_t^{-1+T_2+T_3} , \tag{18}$$

$$\Delta T_s + \Delta T_w + \Delta T_t = C_8 = \Delta T , \tag{19}$$

$$G_s^{2-S_5} D_s^{-1-S_5} L = C_9 = \frac{2 g_c \rho_s \Delta P_s}{S_4 \mu_s^{S_5}} , \tag{20}$$

$$G_t^{2-T_5} L = C_{10} = \frac{2 g_c \rho_t \Delta P_t D_t^{1+T_5}}{T_4 \mu_t^{T_5}} , \tag{21}$$

and

$$A_s N^{-1} D_s^{-1} = C_{11} = \frac{\pi}{4} D_o . \tag{22}$$

The coefficients C_1 through C_{11} are defined by the groupings of input parameters appearing on the extreme right of each multiple equation.

We now reduce the above set of 11 equations to the following single equation in tube-side mass flow,

$$G_t^{E_1} + C_{20} G_t^{E_2} + C_{21} G_t^{E_3} - C_{19} = 0 . \tag{23}$$

The coefficients and exponents appearing in Eq. 23 are, in general, rather complex combinations of the coefficients C_1 through C_{11} and the various coefficients and exponents obtained from Table 3. Details of the elimination process will not be presented here but are available in Appendix A.

Equation 23 may be solved for the tube-side mass flow rate by an iterative process, following which the remaining dependent variables may be determined by a series of back-substitutions.

In any iterative process, the speed of convergence, in fact, perhaps convergence at all, depends on having a good first estimate of the value of the variable being sought. Empirically, the following equation was found to give a good initial estimate for the value of the tube-side mass flow rate.

$$G_t = 0.9\left[\frac{C_{19}}{C_{20} + C_{21}}\right]^{1/E_2} \tag{24}$$

Equation 24 was tested on a wide variety of input parameters and, in most cases, gave an initial value for the tube side flow within 2% of the final iterated value.

Computer Solution

Because of the obvious tedium, and the attendant error-proneness, involved in any sort of desk calculator solution of the above equations, a FORTRAN program was prepared for use on the Call-A-Computer (CAC) time-sharing system. Details of the program operation may be found in the appendices. In particular, a computer-prepared printout of the complete program is presented in Appendix B. Appendix C contains samples of program input and output, together with instructions for use of the program.

Extensions of the Analysis

Although the parametric study presented later in this report assumes an equilateral triangular tube pattern and fused salts in counterflow with equal temperature changes in the two streams, the basic analysis is not, in fact, so limited, as will be shown below.

Other Fluids

Equations 6 and 7 for the convective heat transfer coefficients, although applied in the parametric study only to fused salts, are actually applicable to any fluid having a relatively high Prandtl number. For liquids of very low Prandtl number, such as liquid metals, Eqs. 6 and 7 must be modified. For example, one could employ the Lubarsky-Kaufman relation[6] for the Nusselt number in turbulent flow and the theoretical value of 4.36 in laminar flow. These changes involve only redefining the exponent on the Prandtl number in Eqs. 6 and 7 to be a variable rather than the present constant and extending Table 3.

Tube Patterns

The basic equations, 1 though 11, contain no reference to tube pattern, per se. The implication is that, for a given set of input parameters, the same solution set of dependent variables would be obtained for an equilateral triangular pattern as for, say, a square pattern. This, of course, involves the implicit assumption that the latter spacing is not such as to result in the performance deterioration observed in Figs. 1 and 2.

In order to determine tube spacing, one must employ an auxiliary relation such as Eq. 25,

$$A_s = N(\sqrt{3}S^2/2 - \pi D_o^2/4) \qquad (25)$$

which defines the tube spacing in terms of the shell-side flow area, the number of tubes, and the tube OD for an equilateral triangular pattern.

Other Conditions

Although applied in the parametric study only to a counterflow heat exchanger with equal temperature changes in the two streams, the present analysis may be extended readily, both to parallel flow and to counterflow with unequal temperature changes, by the simple device of properly defining the overall temperature difference. The appropriate quantity is the log mean temperature difference (LMTD), defined by[7]

$$LMTD = \frac{GTD - LTD}{\log_e \frac{GTD}{LTD}} \qquad (26)$$

where GTD is the greater and LTD is the lesser of the two terminal temperature differences between the two streams. When the two temperature differences are equal, the LMTD becomes indeterminate and must be taken as equal to either of the two temperature differences. The existing computer program uses these definitions.

PARAMETRIC STUDY

In this study, the U-tube configuration of Fig. 1 was employed, with the fuel salt flowing axially around the tubes on the shell side and with the inert salt in counterflow inside the tubes. The heat load was kept fixed and equal to that for one of the six heat exchangers for a 2200 Mw(t) reference design reactor.[1] The tube wall material was taken to be INCO 800 and the fuel employed was the lithium-beryllium-thorium-uranium fuel salt in current use for reference design purposes at the time of writing. Two different inert salts, $NaBF_4$ and Flinak, were used in the secondary circuit. The physical properties of the materials used were taken from Refs. 7 and 8 as tabulated in Table 4. The temperature rise in the inert salt and the temperature drop in the fuel in traversing the heat exchanger were kept constant at 250°F.

With a temperature difference between the two fluid streams of 100°F, the heat exchanger characteristics were calculated for each of the two inert salts, using all combinations of three different shell side pressure drops, three different tube side pressure drops, and two different tube diameters. The results are given in Table 5. For one of the tube sizes, the effects of changing the temperature difference between the fluid streams to 125 and 150°F were then investigated for the same set of pressure drops and inert salts used previously. Table 6 summarizes the results from this set of calculations. The input parameter variations used in this study are summarized in Table 7.

Table 4. Reference Design Conditions and the Physical Properties at Design Temperatures for the Materials Used

Reference Design Condition	
Fuel temperature in, °F	1300
Fuel temperature out, °F	1050
Inert salt in, °F	950
Inert salt out, °F	1200
Tube material	INCO 800
Tube thermal conductivity, Btu/hr·ft·F	11.5
Tube OD, in.	0.375
Tube ID, in.	0.3190
Fuel pressure drop, psi	100
Inert salt pressure drop, psi	100

Physical Property	Fluoroborate[a]	Flinak[b]	Fuel[c]
C_p, Btu/lb·F	0.36	0.437	0.325
μ, lb/hr·ft	1.95	12.6	23.5
k, Btu/hr·ft·F	0.266	2.66	0.58
ρ, lb/ft^3	119.0	132.0	208.0
Pr	2.64	2.07	13.1

[a] 92% $NaBF_4$ + 8% NaF

[b] 11.5% NaF + 46.5% LiF + 42% KF

[c] 87% Li_2BeF_3 + 12% ThF_4 + 1% UF_4

Table 5. Effects of Choice of Inert Salt and Tube Diameter on the
for a Full-Scale Molten Salt Breeder Reactor for a Tempe

Inert Salt	Tube OD (in.)	Tube ID (in.)	Pressure Drops		Fuel Side Equivalent Diameter (in.)	Tubes			Volumes			Bundle Weight (lb)	(10-6
			Fuel (psi)	Salt (psi)		Centerline Spacing (in.)	Number	Length (ft)	Fuel (ft^3)	Salt (ft^3)	Tubes (ft^3)		
$NaBF_4$	0.3125	0.2665	100	100	0.2823	0.4106	4944	31.5	74.9	60.3	22.6	34757	
				150	0.3231	0.4244	4219	35.5	82.5	58.0	21.7	35598	
				200	0.3557	0.4352	3774	38.7	88.6	56.6	21.2	36420	
			150	100	0.2466	0.3981	4806	29.9	60.4	55.7	20.9	30275	
				150	0.2823	0.4106	4095	33.6	66.3	53.3	20.0	30754	
				200	0.3107	0.4203	3659	36.6	71.0	51.9	19.5	31281	
			200	100	0.2241	0.3900	4716	28.9	52.1	52.8	19.8	27634	
				150	0.2565	0.4016	4015	32.5	57.0	50.5	18.9	27911	
				200	0.2823	0.4106	3586	35.3	60.9	49.0	18.4	28276	
	0.3750	0.3190	100	100	0.3374	0.4922	3498	40.0	96.6	77.7	29.7	45099	
				150	0.3862	0.5088	2986	45.2	106.5	74.8	28.6	46238	
				200	0.4251	0.5216	2672	49.3	114.5	73.1	27.9	47335	
			150	100	0.2947	0.4773	3403	38.1	78.2	72.0	27.5	39417	
				150	0.3374	0.4922	2902	42.9	85.9	69.1	26.4	40091	
				200	0.3714	0.5038	2594	46.7	92.1	67.3	25.7	40811	
			200	100	0.2678	0.4676	3343	36.9	67.5	68.4	26.1	36064	
				150	0.3065	0.4814	2848	41.5	74.0	65.5	25.0	36478	
				200	0.3374	0.4922	2544	45.1	79.2	63.7	24.3	36989	
Flinak	0.3125	0.2665	100	100	0.2899	0.4132	4444	28.1	61.7	48.4	18.2	28871	
				150	0.3318	0.4273	3820	32.1	69.4	47.5	17.8	30175	
				200	0.3652	0.4383	3434	35.4	75.6	47.0	17.6	31291	
			150	100	0.2532	0.4004	4299	26.5	49.2	44.1	16.6	24842	
				150	0.2899	0.4132	3692	30.2	55.1	43.2	16.2	25770	
				200	0.3190	0.4231	3316	33.2	59.9	42.7	16.0	26584	
			200	100	0.2301	0.3921	4206	25.5	42.0	41.5	15.6	22485	
				150	0.2634	0.4040	3609	29.0	47.0	40.6	15.2	23204	
				200	0.2899	0.4132	3240	31.9	51.0	40.0	15.0	23849	
	0.3750	0.3190	100	100	0.3464	0.4953	3153	35.9	80.3	62.9	24.0	37771	
				150	0.3966	0.5123	2711	41.1	90.4	61.8	23.6	39493	
				200	0.4365	0.5253	2437	45.2	98.4	61.2	23.4	40962	
			150	100	0.3026	0.4801	3055	34.0	64.2	57.6	22.0	32647	
				150	0.3464	0.4953	2624	38.8	72.1	56.4	21.6	33888	
				200	0.3813	0.5072	2358	42.6	78.4	55.8	21.3	34969	
			200	100	0.2750	0.4702	2992	32.7	55.1	54.3	20.8	29644	
				150	0.3148	0.4843	2569	37.3	61.6	53.1	20.3	30616	
				200	0.3464	0.4953	2307	41.0	66.9	52.4	20.0	31479	

Proportions of a Series of Fuel-to-Inert-Salt Heat Exchangers
rature Change of 100°F in the Fuel and Salt Circuits

Mass Flows			Flow Velocities		Reynolds Numbers		Pumping Power		Temperature Drops		
Fuel ($\times$ lb/hr·ft^2)	Salt (10^{-6} $\times$ lb/hr·ft^2)	Ratio Salt/Fuel	Fuel (ft/sec)	Salt (ft/sec)	Fuel	Salt	Fuel (hp)	Salt (hp)	Film Fuel Side (F°)	Wall (F°)	Film Salt Side (F°)
6.497	7.263	1.1179	8.7	17.0	6504	82720	540	850	47.0	17.7	35.2
6.652	8.512	1.2797	8.9	19.9	7623	96947	540	1275	49.3	18.4	32.3
6.757	9.517	1.4084	9.0	22.2	8522	108383	540	1700	50.9	18.9	30.3
7.652	7.473	0.9766	10.2	17.4	6692	85109	811	850	43.5	19.2	37.3
7.845	8.770	1.1179	10.5	20.5	7853	99880	811	1275	45.7	20.0	34.3
7.976	9.813	1.2304	10.7	22.9	8788	111764	811	1700	47.2	20.6	32.2
8.582	7.615	0.8873	11.5	17.8	6819	86722	1081	850	41.0	20.2	38.7
8.806	8.944	1.0157	11.8	20.9	8009	101866	1081	1275	43.2	21.2	35.6
8.959	10.015	1.1179	12.0	23.4	8968	114058	1081	1700	44.7	21.8	33.5
6.403	7.166	1.1190	8.6	16.7	7661	97683	540	850	45.7	20.0	34.3
6.553	8.394	1.2809	8.8	19.6	8975	114428	540	1275	47.8	20.8	31.4
6.654	9.381	1.4099	8.9	21.9	10030	127886	540	1700	49.3	21.3	29.4
7.534	7.364	0.9775	10.1	17.2	7874	100396	811	850	42.1	21.6	36.2
7.719	8.638	1.1190	10.3	20.2	9235	117752	811	1275	44.2	22.5	33.2
7.845	9.662	1.2316	10.5	22.6	10330	131713	811	1700	45.7	23.1	31.2
8.443	7.498	0.8882	11.3	17.5	8017	102221	1081	850	39.7	22.7	37.6
8.658	8.802	1.0167	11.6	20.5	9411	119995	1081	1275	41.7	23.7	34.5
8.804	9.852	1.1190	11.8	23.0	10533	134301	1081	1700	43.2	24.4	32.4
7.040	6.658	0.9456	9.4	14.0	7237	11734	540	631	55.2	22.1	22.7
7.155	7.745	1.0824	9.6	16.3	8419	13651	540	947	57.0	22.5	20.5
7.232	8.616	1.1914	9.7	18.1	9366	15186	540	1263	58.3	22.7	19.0
8.330	6.881	0.8261	11.1	14.5	7480	12128	811	631	51.5	24.2	24.3
8.474	8.014	0.9456	11.3	16.9	8711	14124	811	947	53.3	24.7	21.9
8.572	8.921	1.0408	11.4	18.8	9697	15724	811	1263	54.6	25.1	20.4
9.371	7.033	0.7505	12.5	14.8	7645	12397	1081	631	48.9	25.7	25.3
9.541	8.197	0.8591	12.7	17.2	8910	14448	1081	947	50.7	26.4	22.9
9.655	9.130	0.9456	12.9	19.2	9924	16092	1081	1263	51.9	26.7	21.4
6.918	6.548	0.9466	9.2	13.8	8499	13815	540	631	53.3	24.7	22.0
7.029	7.616	1.0835	9.4	16.0	9885	16068	540	947	55.0	25.2	19.8
7.103	8.471	1.1926	9.5	17.8	10994	17872	540	1263	56.2	25.4	18.4
8.173	6.758	0.8269	10.9	14.2	8771	14258	811	631	49.6	27.0	23.4
8.312	7.868	0.9466	11.1	16.6	10211	16599	811	947	51.3	27.6	21.1
8.405	8.757	1.0418	11.2	18.4	11365	18475	811	1263	52.5	27.9	19.6
9.184	6.900	0.7513	12.3	14.5	8956	14558	1081	631	47.0	28.6	24.4
9.347	8.039	0.8600	12.5	16.9	10433	16960	1081	947	48.7	29.3	22.1
9.457	8.952	0.9466	12.6	18.8	11618	18886	1081	1263	49.8	29.7	20.5

Table 6. Effects of Choice of Temperature Change in the F
Intermediate Heat Exchangers for a Full-

ΔT (°F)	Inert Salt	Pressure Drops		Fuel Side Equivalent Diameter (in.)	Tubes			Volumes			Bundle Weight (lb)	
		Fuel (psi)	Salt (psi)		Centerline Spacing (in.)	Number	Length (ft)	Fuel (ft^3)	Salt (ft^3)	Tubes (ft^3)		Fuel (10^{-6} × lb/hr·ft^2)
125	$NaBF_4$	100	100	0.2823	0.4106	4456	26.1	56.0	45.1	16.9	25980	7.209
			150	0.3231	0.4244	3803	29.4	61.7	43.4	16.3	26630	7.379
			200	0.3557	0.4352	3403	32.1	66.3	42.3	15.9	27258	7.494
		150	100	0.2466	0.3981	4334	24.8	45.2	41.7	15.6	22666	8.486
			150	0.2823	0.4106	3694	27.9	49.7	40.0	15.0	23046	8.697
			200	0.3107	0.4203	3302	30.4	53.2	38.9	14.6	23456	8.840
		200	100	0.2241	0.3900	4255	24.0	39.0	39.6	14.8	20713	9.513
			150	0.2565	0.4016	3624	27.0	42.7	37.9	14.2	20942	9.758
			200	0.2823	0.4106	3237	29.4	45.7	36.8	13.8	21230	9.924
	Flinak	100	100	0.2899	0.4132	4012	23.4	46.4	36.4	13.6	21683	7.798
			150	0.3318	0.4273	3449	26.7	52.1	35.7	13.4	22673	7.924
			200	0.3652	0.4383	3101	29.4	56.8	35.3	13.3	23517	8.009
		150	100	0.2352	0.4004	3885	22.1	37.0	33.2	12.5	18700	9.219
			150	0.2899	0.4132	3336	25.2	41.5	32.5	12.2	19409	9.377
			200	0.3190	0.4231	2997	27.7	45.1	32.1	12.1	20028	9.484
		200	100	0.2301	0.3921	3803	21.2	31.7	31.3	11.7	16953	10.366
			150	0.2634	0.4040	3264	24.2	35.5	30.6	11.5	17506	10.551
			200	0.2899	0.4132	2931	26.6	38.5	30.2	11.3	17999	10.676
150	$NaBF_4$	100	100	0.2823	0.4106	4095	22.4	44.2	35.6	13.3	20502	7.845
			150	0.3231	0.4244	3496	25.3	48.7	34.3	12.8	21029	8.028
			200	0.3557	0.4352	3128	27.6	52.4	33.5	12.5	21534	8.152
		150	100	0.2466	0.3981	3984	21.3	35.7	32.9	12.4	17912	9.230
			150	0.2823	0.4106	3397	24.0	39.3	31.6	11.9	18226	9.457
			200	0.3107	0.4203	3037	26.2	42.1	30.8	11.6	18559	9.611
		200	100	0.2241	0.3900	3913	20.7	30.9	31.3	11.7	16384	10.344
			150	0.2565	0.4016	3334	23.2	33.8	30.0	11.2	16579	10.607
			200	0.2823	0.4106	2978	25.3	36.2	29.2	10.9	16816	10.786
	Flinak	100	100	0.2899	0.4132	3692	20.1	36.7	28.8	10.8	17180	8.474
			150	0.3318	0.4273	3174	23.0	41.3	28.3	10.6	17970	8.610
			200	0.3652	0.4383	2854	25.3	45.0	28.0	10.5	18644	8.701
		150	100	0.2532	0.4004	3577	19.0	29.4	26.4	9.9	14844	10.012
			150	0.2899	0.4132	3073	21.7	33.0	25.8	9.7	15414	10.182
			200	0.3190	0.4231	2761	23.9	35.8	25.5	9.6	15910	10.296
		200	100	0.2301	0.3921	3503	18.3	25.2	24.9	9.3	13476	11.251
			150	0.2634	0.4040	3007	20.9	28.2	24.3	9.1	13922	11.450
			200	0.2899	0.4132	2701	22.9	30.6	24.0	9.0	14319	11.585

uel and Inert Salt on the Proportions of a Series of
Scale Molten Salt Breeder Reactor

Mass Flows		Flow Velocities		Reynolds Numbers		Pumping Power		Temperature Drops		
Salt (10^{-6} × lb/hr·ft^2)	Ratio Salt/Fuel	Fuel (ft/sec)	Salt (ft/sec)	Fuel	Salt	Fuel (hp)	Salt (hp)	Film Fuel Side (°F)	Wall (°F)	Film Salt Side (°F)
8.059	1.1179	9.6	18.8	7216	91781	540	850	57.9	23.7	43.4
9.442	1.2797	9.9	22.0	8455	107536	540	1275	60.6	24.6	39.7
10.554	1.4084	10.0	24.6	9451	120200	540	1700	62.6	25.2	37.2
8.287	0.9766	11.3	19.3	7421	94377	811	850	53.5	25.6	45.9
9.722	1.1179	11.6	22.7	8706	110720	811	1275	56.2	26.7	22.7
10.876	1.2304	11.8	25.4	9739	123868	811	1700	58.0	27.5	39.5
8.440	0.8873	12.7	19.7	7558	96127	1081	850	50.4	27.0	47.6
9.911	1.0157	13.0	23.1	8875	112872	1081	1275	53.0	28.2	43.8
11.094	1.1179	13.3	25.9	9935	126352	1081	1700	54.9	29.0	41.1
7.374	0.9456	10.4	15.5	8016	12998	540	631	67.7	29.4	27.9
8.578	1.0824	10.6	18.1	9324	15118	540	947	69.9	29.9	25.1
9.541	1.1914	10.7	20.1	10371	16817	540	1263	71.4	30.2	23.3
7.616	0.8261	12.3	16.0	8278	13423	811	631	63.1	32.2	29.7
8.867	0.9456	12.5	18.7	9639	15629	811	947	65.3	32.8	26.9
9.870	1.0408	12.7	20.8	10729	17397	811	1263	66.8	33.3	25.0
7.780	0.7505	13.8	16.4	8457	13712	1081	631	59.8	34.1	31.0
9.065	0.8591	14.1	19.1	9854	15977	1081	947	62.0	34.9	28.1
10.095	0.9456	14.3	21.2	10974	17793	1081	1263	63.5	35.4	26.1
8.770	1.1179	10.5	20.5	7853	99880	540	850	68.6	30.1	51.4
10.273	1.2797	10.7	24.0	9199	116998	540	1275	71.8	31.2	47.0
11.481	1.4084	10.9	26.8	10281	130756	540	1700	74.0	31.9	44.0
9.014	0.9766	12.3	21.0	8071	102655	811	850	63.3	32.4	54.3
10.572	1.1179	12.6	24.7	9467	120398	811	1275	66.4	33.8	49.8
11.825	1.2305	12.8	27.6	10589	134671	811	1700	68.6	34.7	46.7
9.178	0.8873	13.8	21.4	8218	104523	1081	850	59.6	34.1	56.3
10.773	1.0157	14.2	25.1	9647	122693	1081	1275	62.7	35.6	51.7
12.057	1.1179	14.4	28.1	10797	137318	1081	1700	64.8	36.6	48.6
8.014	0.9456	11.3	16.9	8711	14124	540	631	80.0	37.1	32.9
9.320	1.0824	11.5	19.6	10131	16427	540	947	82.6	37.8	29.7
10.366	1.1914	11.6	21.8	11268	18271	540	1263	84.3	38.1	27.5
8.270	0.8261	13.4	17.4	8990	14577	811	631	74.4	40.5	35.0
9.628	0.9456	13.6	20.3	10466	16970	811	947	77.0	41.4	31.7
10.716	1.0408	13.8	22.6	11648	18888	811	1263	78.7	41.9	29.4
8.444	0.7505	15.0	17.8	9179	14884	1081	631	70.5	43.0	36.5
9.838	0.8591	15.3	20.7	10693	17339	1081	947	73.0	43.9	33.1
10.954	0.9456	15.5	23.1	11908	19308	1081	1263	74.7	44.5	30.7

Table 7. Summary of Input Parameter Variations Used in Parametric Study

Pressure Drops (psi)		Tube OD (in.)	Inert Salts	Temperature Difference (°F)
Shell Side	Tube Side			
100, 150, 200	100, 150, 200	5/16, 3/8	$NaBF_4$, Flinak	100
100, 150, 200	100, 150, 200	5/16	$NaBF_4$, Flinak	125, 150

The principal results of the parametric calculations are summarized in the series of curves presented in Figs. 4 through 9. Figures 4 through 6 show the effects of pressure drop, tube size, and inert salt on the number of tubes, the tube length, and the heat exchanger fuel inventory for a temperature difference of 100°F between the fuel and inert salt. Figures 7 through 9 show the effects on the same dependent variables of changes in pressure drop and temperature difference between the two fluids for each of the two inert salts, with a tube OD of 5/16 in.

Examination of Fig. 4 reveals that, if one decreases tube OD from 3/8 to 5/16 in., the number of tubes in the bundle increases by approximately 40% for either inert salt, all other things being equal. It can be seen that changes in the tube side, or inert salt, pressure drop are much more effective in reducing the number of tubes in the bundle than the corresponding change in the shell side, or fuel, pressure drop. A change in the salt pressure drop from 100 to 200 psi reduces the number of tubes by approximately 25%, whereas the same change in the fuel pressure drop produces a reduction of only about 5%. For a typical set of conditions, changing the inert salt from $NaBF_4$ to Flinak produces a reduction in the number of tubes by approximately 10%.

For the same set of changes, Fig. 5 shows the resulting effects on tube length. Reducing the tube OD to 5/16 in. yields, for either inert salt and for a given set of pressure drops, a reduction in the tube length of approximately 20%. As before, an increase in fuel pressure drop produces a reduction in the dependent variable, in this case, about 10% in

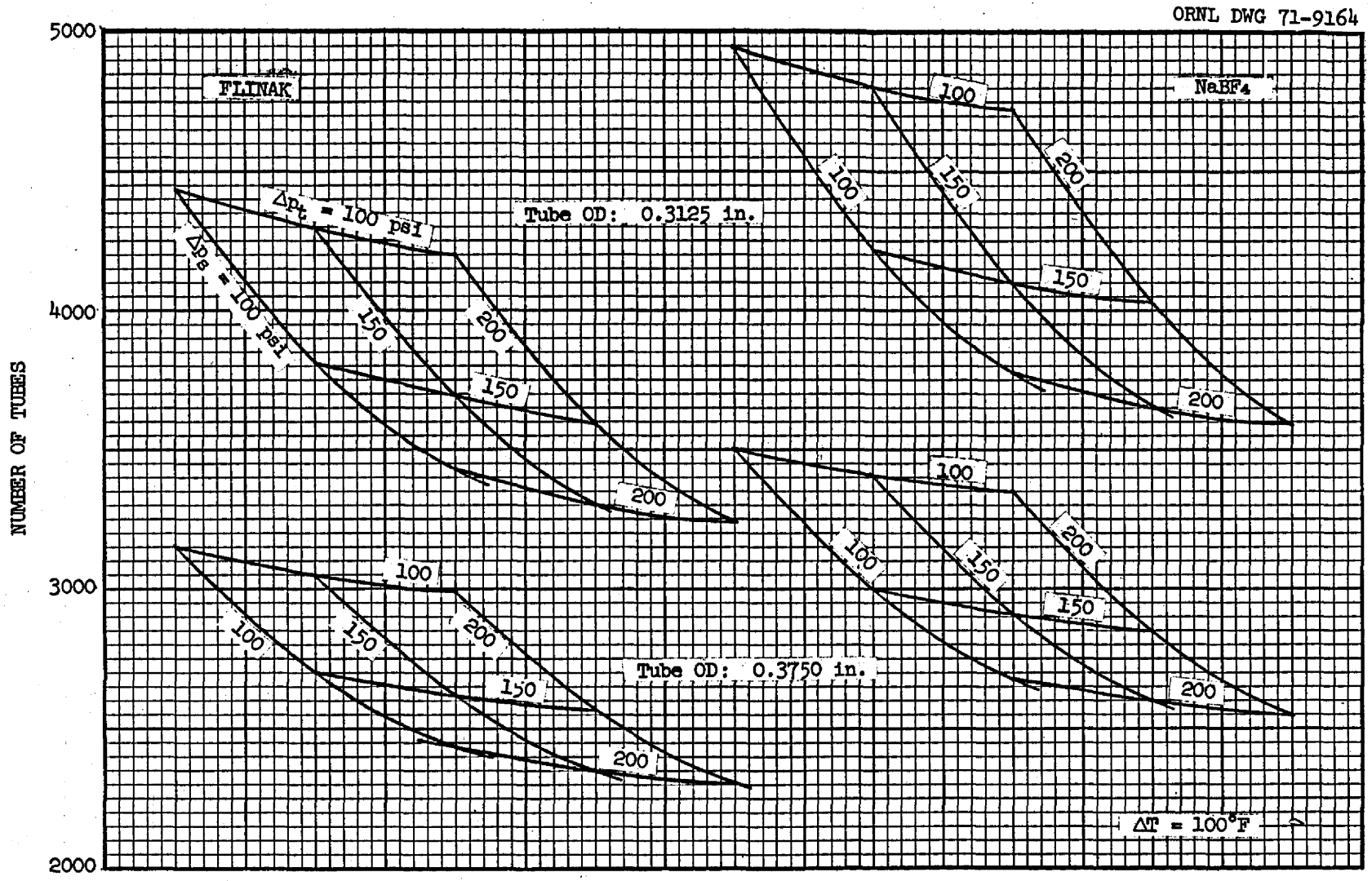

Fig. 4. Number of Tubes in a Bundle as a Function of Shell and Tube Side Pressure Drops for Two Tube Sizes and Two Inert Salts.

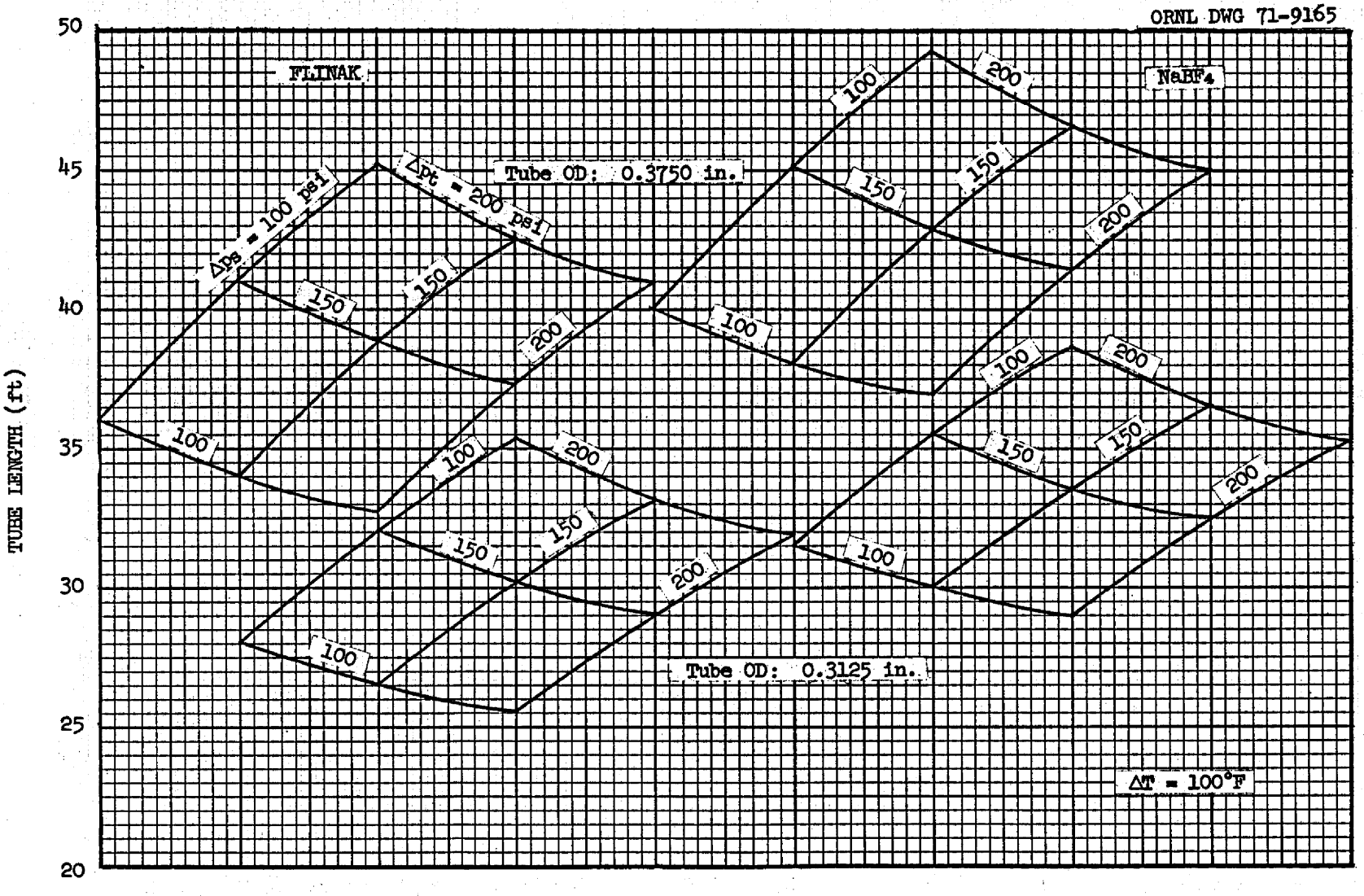

Fig. 5. Tube Bundle Length as a Function of Shell and Tube Side Pressure Drops for Two Tube Sizes and Two Inert Salts.

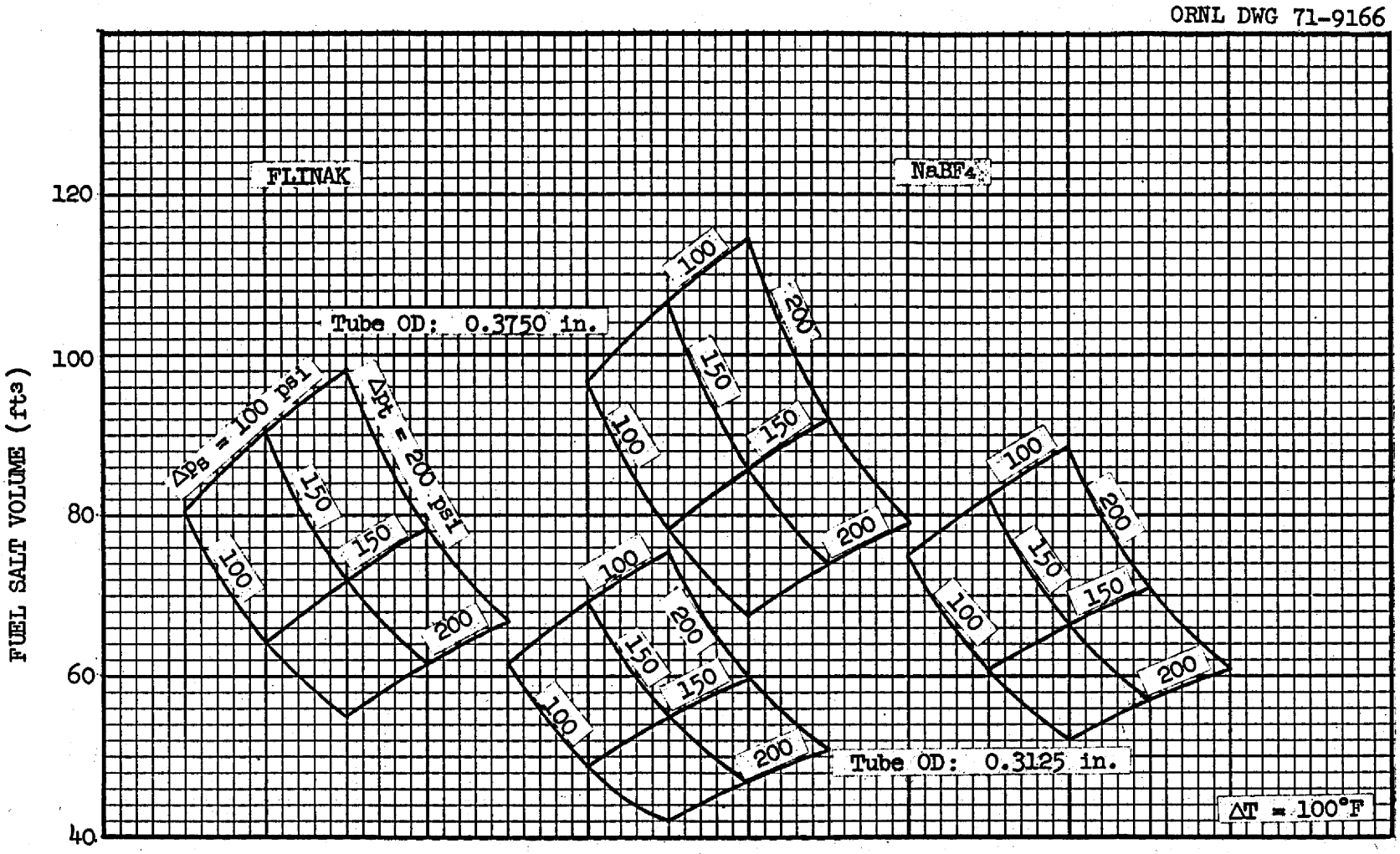

Fig. 6. Fuel Salt Volume in Tube Bundle as a Function of Shell and Tube Side Pressure Drops for Two Tube Sizes and Two Inert Salts.

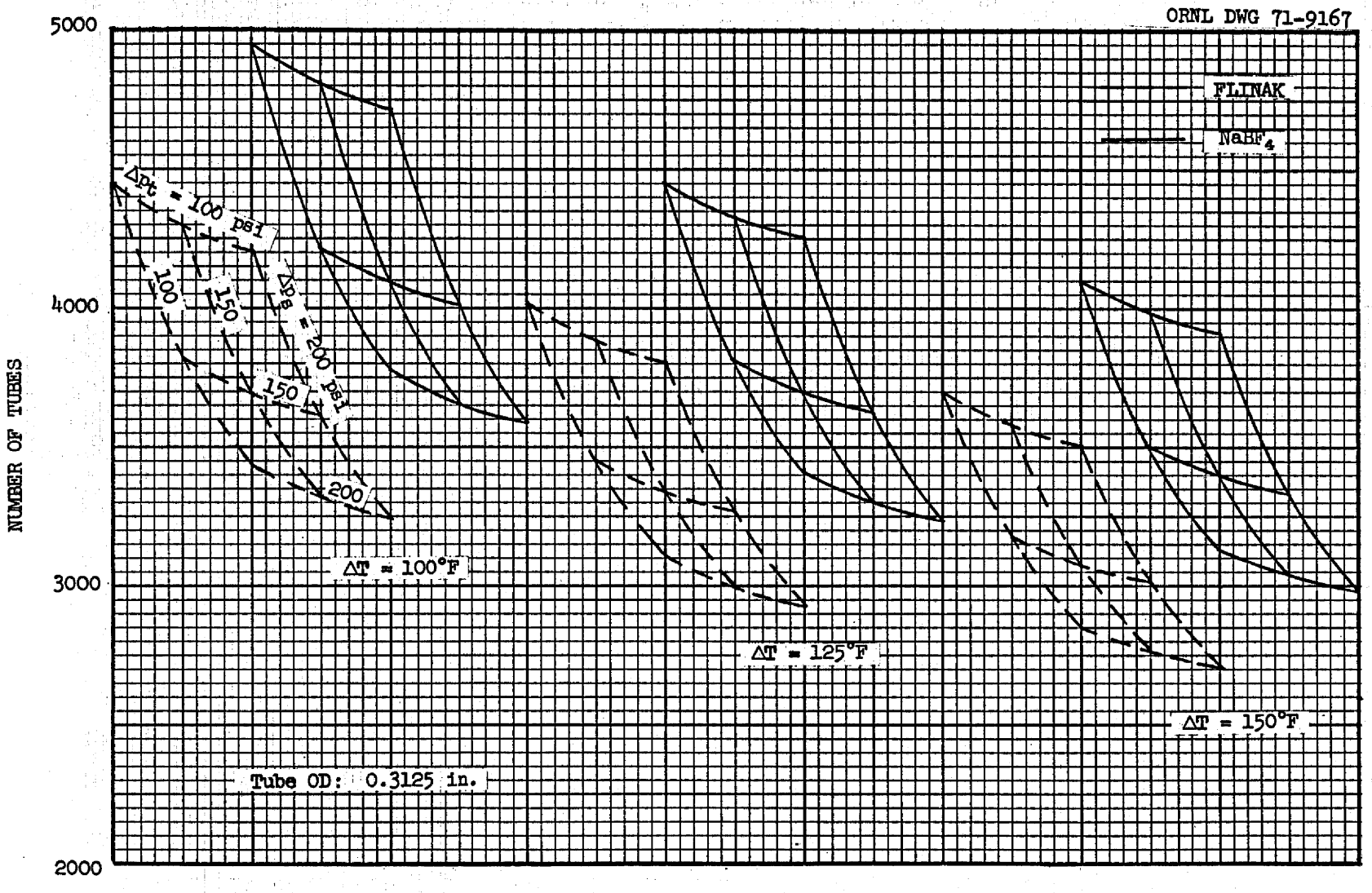

Fig. 7. Number of Tubes in a Bundle as a Function of Shell and Tube Side Pressure Drops for Three Temperature Differences and Two Inert Salts.

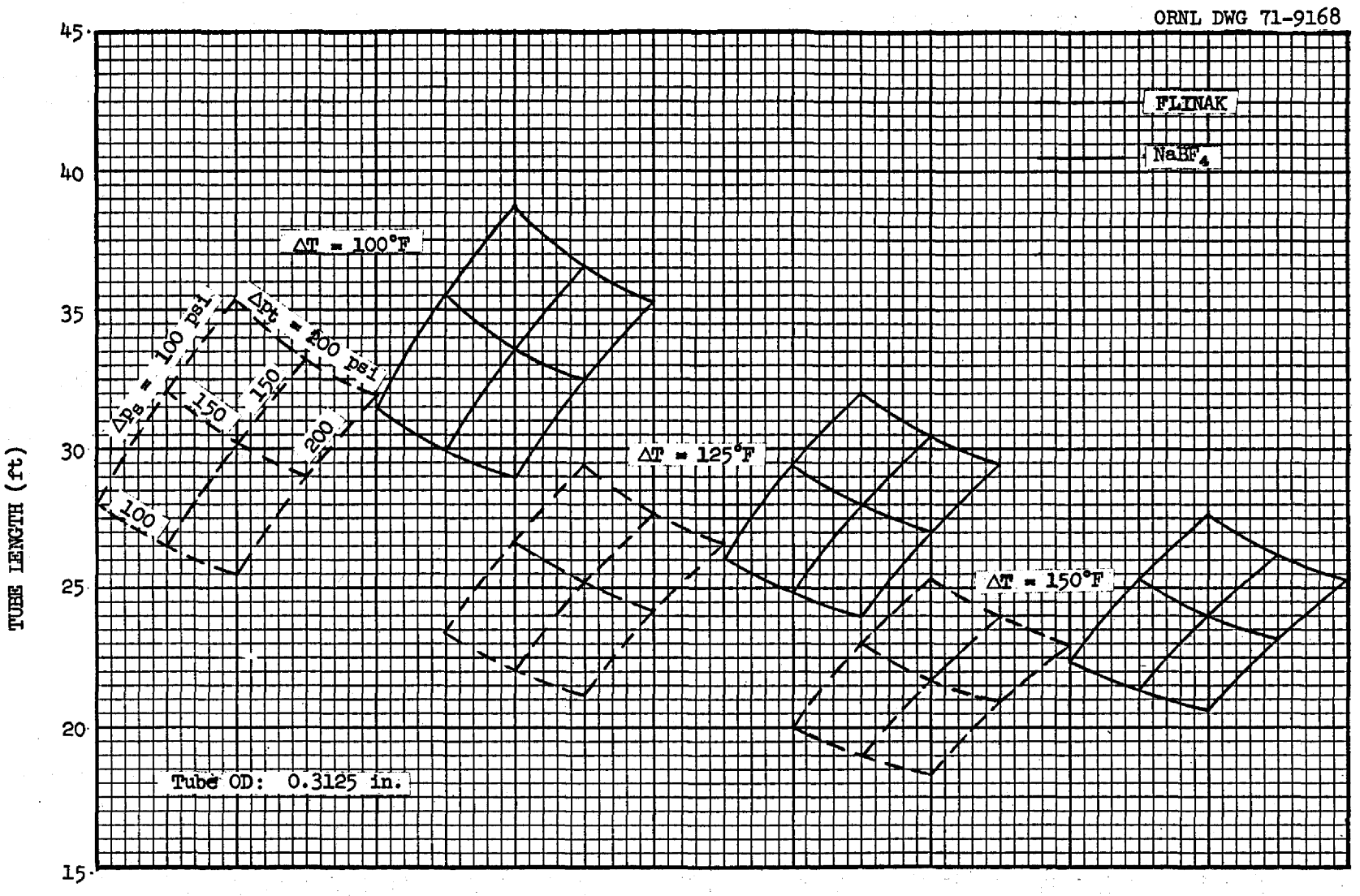

Fig. 8. Tube Bundle Length as a Function of Shell and Tube Size Pressure Drops for Three Temperature Differences and Two Inert Salts.

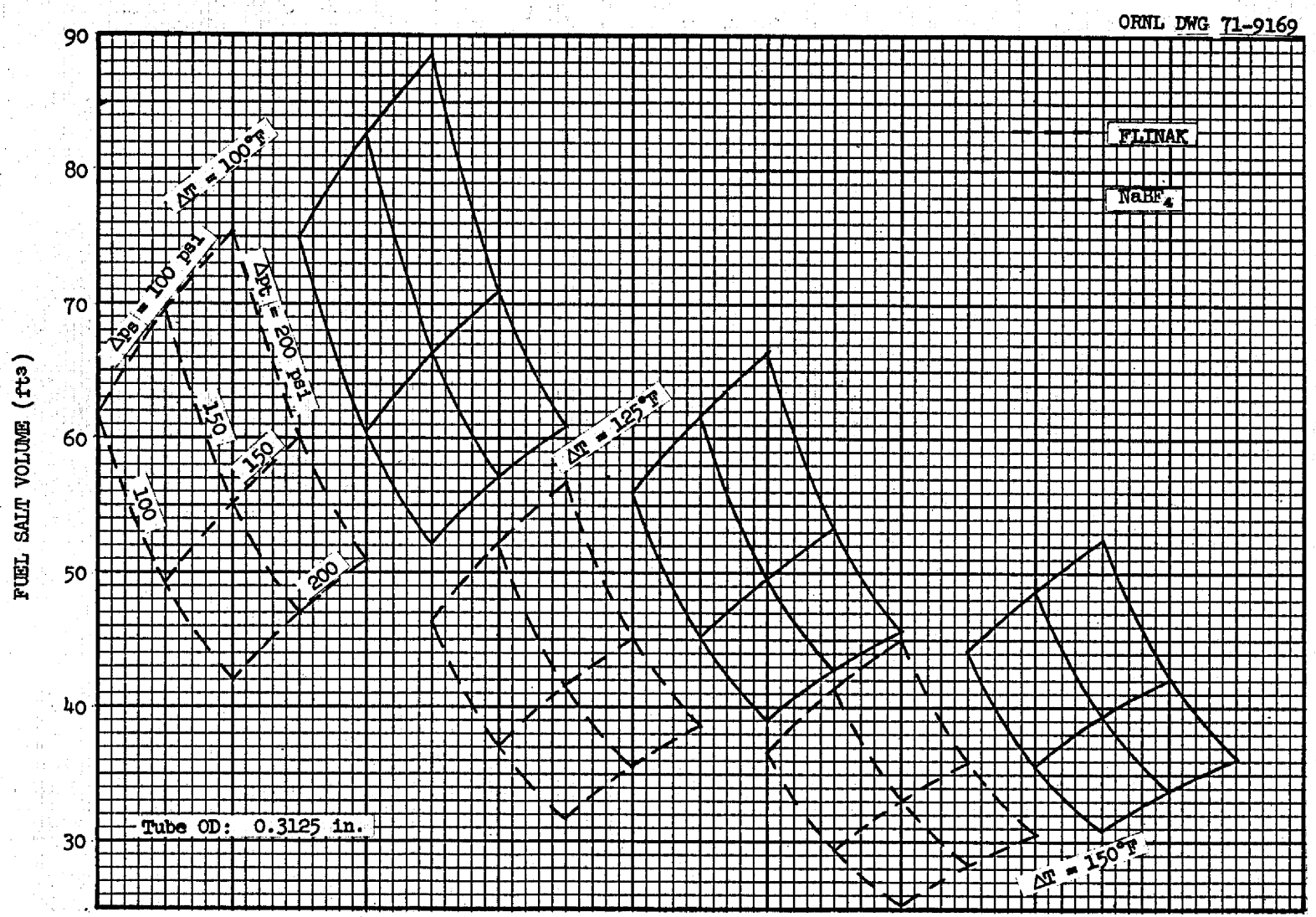

Fig. 9. Fuel Salt Volume in Tube Bundle as a Function of Shell and Tube Side Pressure Drops for Three Temperature Differences and Two Inert Salts.

the length. We note, however, that an increase in salt pressure drop has the opposite effect, a doubling of the pressure drop yielding nearly 25% increase in the tube length. With all other conditions fixed, a change of inert salt from $NaBF_4$ to Flinak gives a reduction in tube length of about 10%.

The heat exchanger fuel inventory, a dependent variable of major interest, is shown in Fig. 6. For a given set of conditions, the prescribed reduction in tube OD yields a corresponding reduction in fuel volume of about 25%. Increasing the fuel pressure drop, as before, yields a substantial savings in fuel inventory of nearly 30%. In contrast, however, increasing the salt pressure drop from 100 to 200 psi produces an increase in fuel volume of about 20%. Replacing the inert salt in the secondary circuit with Flinak reduces the heat exchanger fuel inventory by about 20%.

Figures 7 through 9 are intended, primarily, to show the effects of increasing the temperature difference between the two fluid streams. The tube diameter used is the smaller one, 5/16 in. Figure 7 shows that increasing the temperature difference from 100 to 125°F yields a decrease in the number of tubes of approximately 10%. A further increase in the temperature difference to 150°F yields only an additional 5% reduction, giving an overall reduction in the number of tubes of approximately 15% from the 100°F temperature difference reference condition. For the same changes in temperature difference between the two fluids, one observes from Fig. 8 that the corresponding reductions in tube length are 15 and 30%, respectively. Finally, as can be seen from Fig. 9, major savings in fuel inventory can be effected if the temperature difference between the salt streams can be increased. Increasing the difference from 100 to 125°F results in a 25% reduction in fuel inventory and a 150°F difference yields an overall reduction of 40% in the fuel salt volume.

As discussed earlier, a temperature difference of 125°F would probably pose no problems with thermal stresses, but a temperature difference of 150°F might give trouble and would require extensive proof testing because it is difficult to evaluate precisely some of the modes of failure that might prove important.

Table 1 is a concise summary of the information contained in Figs. 4 through 9 as discussed in the preceding paragraphs. This table can be

used to make rough estimates of the effects on the number of tubes, the tube length, and the fuel volume of arbitrary combinations of changes in the listed parameters. For example, if we were, simultaneously, to reduce tube OD from 3/8 in. to 5/16 in. and raise the temperature difference from 100°F to 150°F, the relative number of tubes would be approximated by

$$(1.40)(0.85) = 1.19$$

the relative tube length would be

$$(0.80)(0.70) = 0.56$$

and the relative fuel volume would be

$$(0.75)(0.60) = 0.45$$

Actually, some of the effects are interrelated in such a way that taking advantage of one effect may reduce the effect of another, hence it is best to use the charts of Figs. 4 to 9 when estimating the combined effects of several simultaneous changes. If these are not applicable, new calculations can be made using the program appended at the end of this report.

From the equations in the analysis section of this report, it can be shown that the pumping power in either fluid circuit, for a given heat load and fluid temperature change, depends only on the salt properties, the temperature change, and the pressure drop in that circuit. Then, for a given fuel salt and temperature change, the ratio of the total heat exchanger pumping powers for two different inert salts depends only on the ratio of the inert salt pressure drop to the fuel pressure drop. This relation is shown in Fig. 10 for a change in inert salt from $NaBF_4$ to Flinak, the total pumping power ratio being plotted as a function of the pressure drop ratio. Over the pressure drop ratio range of about 0.5 to 2.0, the corresponding saving in total heat exchanger pumping power is from approximately 10 to about 20%.

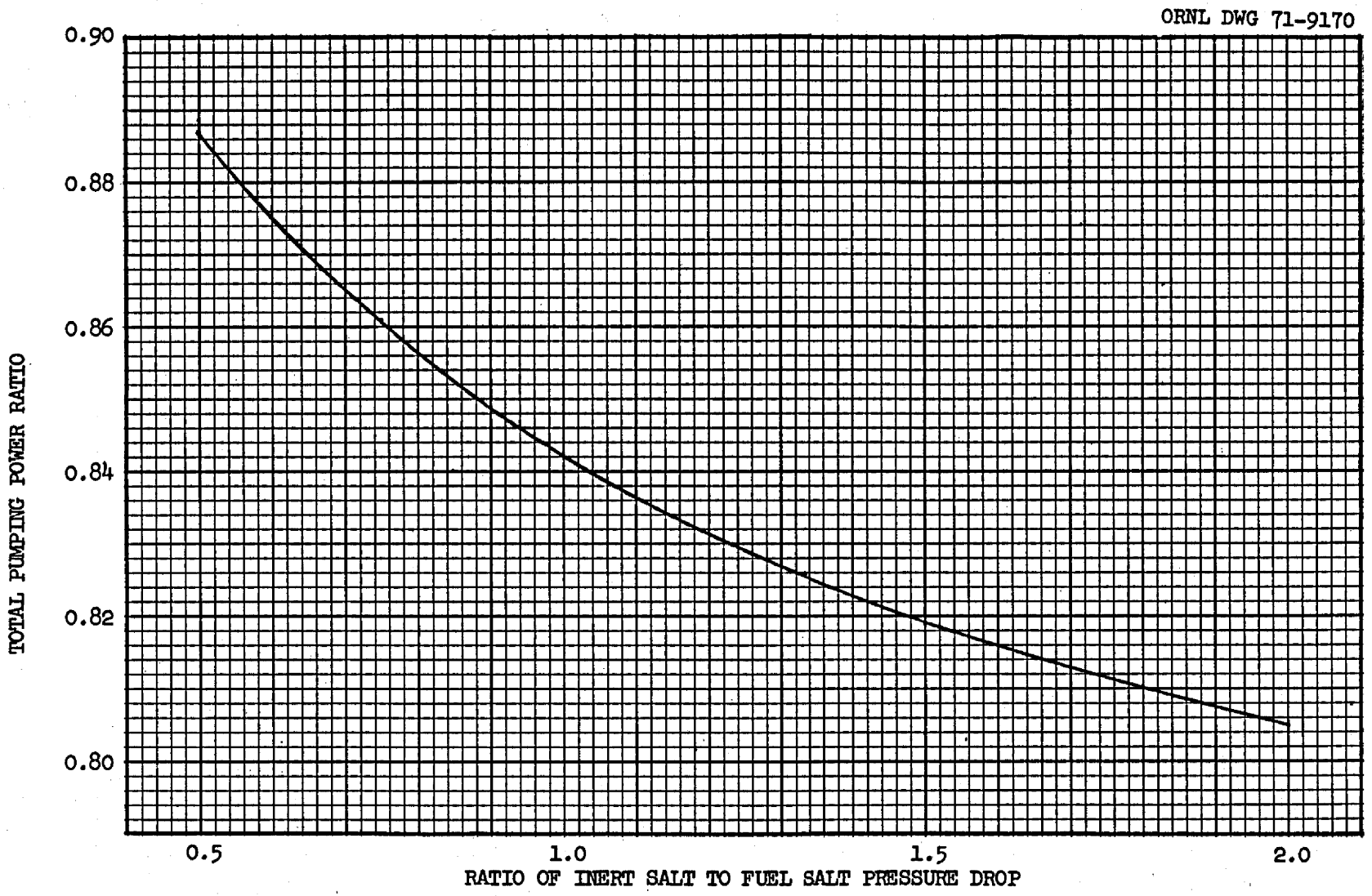

Fig. 10. Effect of Pressure Drop Ratio on the Reduction of Total Pumping Power with a Change in Inert Salt from $NaBF_4$ to Flinak.

CHOICE OF INERT SALT

In recent years sodium fluoroborate has been the favored candidate for use as the inert salt in the intermediate heat transfer fluid system of the MSBR. However, the writers felt that heat transfer considerations make it worthwhile to review the possible advantages and disadvantages of another candidate, Flinak, an inert salt that was employed in many tests carried out under the ANP program.

Materials Compatibility Considerations

The mass transfer and corrosion problems associated with the use of both Flinak and fluoroborate salt were discussed at some length with J. H. DeVan who kindly provided most of the material presented here. The materials compatibility tests cited in this section are best understood if considered in historical perspective. It should be remembered that under the ANP program some difficulties with corrosion and mass transfer were observed in the Inconel loops operated with fluoride salts, particularly those containing UF_4. As a consequence, a series of alloys was tested to develop something having better corrosion resistance than Inconel. Around 40 individual thermal convection loops were built of different nickel-molybdenum alloys containing various additions of titanium, aluminum, chromium, niobium, vanadium, and iron. These loops were tested at 815°C for periods of time ranging from 500 to 1000 hr. All of the loops except those containing large amounts of titanium and aluminum were essentially unaffected by the fuel salt. The development of INOR-8 and Hastelloy-N was an outgrowth of this work, which is reported in Refs. 9 through 16. Unfortunately, no recent tests have been run with Flinak in the latest and most promising alloy, Hastelloy-N, but it is believed that the results of such tests would be more favorable than any of the earlier work because of improved techniques for purifying the salt and loading it in the loop. Note also that Hastelloy-N should be more corrosion resistant than the Hastelloy-B, and elimination of the UF_4 (added to the Flinak in the thermal convection loop tests) should reduce the tendency of the salt to attack the structural material.

The results of tests with thermal convection and forced convection loops both with Flinak and with fluoroborate salt are summarized in Table 8. Note that three of the Flinak forced convection loops were operated at over 1700°F with a temperature drop in the salt circuit ranging from 365 to 450°F, a very severe combination of conditions. While the first of these showed some tendency to form subsurface voids as a result of solid state diffusion and selective leaching of iron from the alloy, this effect was not noticable in the other two loops.

The test experience with fluoroborate salt was discussed with J. W. Koger who supplied the information summarized in the lower portion of Table 8. The data fall into two major sets. The first set was carried out with the first fluoroborate salt to become available.[17] This material contained about 2000 ppm of oxygen because this was the highest purity obtainable with the usual fluoride purification process; evolution of BF_3 prevented a further reduction in impurities. (The vapor pressure of BF_3 at 1125°F is 160 mm whereas the vapor pressure of the Flinak is less than 1 mm at the same temperature.) As a consequence of the high concentration of impurities in the first batch of fluoroborate salt, the Croloy 9 Cr-1 Mo loop was attacked very rapidly so that operation had to be terminated after about 1400 hr (Ref. 17). The Hastelloy-N loop, however, was only lightly attacked — at a rate equivalent to about 2 mils/yr — but the cold leg began to plug with Na_3CeF_6 so that operation was terminated at the end of 10,000 hr (Ref. 17).

The second series of tests was run with a more highly purified fluoroborate salt having a nominal contamination level of 500 ppm of oxygen.[18] Three of these loops have been operated for over 20,000 hr with no apparent signs of plug formation or other serious ill effects.[19]

Melting Point

In the design and operation of any high-temperature liquid system it is always advantageous to reduce the melting point of the fluid employed in order to ease the problems of preheating, filling, and draining the system. Further, if the system is to include a steam generator, it would be highly desirable to be able to make use of a molten salt whose melting

Table 8. Summary of Thermal and Forced Convection Loop Tests Carried Out with Flinak and with $NaBF_4$

Molten Salt	Mode of Circulation	Structural Material	Peak Metal Temperature (°F)	ΔT (°F)	Test Duration (hr)	Results
Flinak (46.5 LiF + 11.5 NaF + 42 KF)	Thermal convection	Inconel	1125	100	1000[6]	Attack <1 mil
		Inconel	1050	100	4360[7]	Attack ≤2 mils
		Inconel	1250	100	4373[8]	Attack to 13 mils in the form of subsurface voids along grain boundaries; after-test chemistry indicated that initial salt loading was contaminated with moisture
		INOR-8	1125	100	1000[9]	No attack
		INOR-8	1250	100	1340[9]	No attack
		INOR-8	1250	100	8760[10]	Attack <1 mil
Flinak + 2.5% UF_4	Forced convection	Inconel	1200	100	8760	System troubles led to three changes of fluid charge in course of tests; maximum attack was 8 mils in hot zone
		17 Mo, 6 Fe Ba 1 Ni	1760	450	1000	Void formation to depth of ~4 mils
		Hastelloy B	1767	410	1000	Pits present in as-received tubing were slightly accentuated; no noticeable void formation
		Hastelloy B	1710	365	1000	Do above; a few metal crystals noted at pump bowl exit
92 $NaBF_4$ + 8 NaF	Thermal convection	Croloy 9 Cr-1 Mo	1125	270	~1400	Initial O_2 2000 ppm; severe attack
		Hastelloy N	1125	270	10,000	Initial O_2 2000 ppm; attack ~2 mil; loop partially plugged by deposit of Na_3CrF_6
$NaBF_4$-NaF (92-8)	Thermal convection	Hastelloy N	607	260	20,380	Test continuing
$NaBF_4$-NaF (92-8)	Thermal convection	Hastelloy N	607	300	28,955	Test continuing
LiF-BeF_2-ThF_4 (73-2-25)	Thermal convection	Hastelloy N	677	130	17,880	Test continuing
LiF-BeF_2-UF_4 (65.5-34.0-0.5)	Thermal convection	Hastelloy N	704	340	22,240	Test continuing
$NaBF_4$-NaF (92-8) plus steam additions	Thermal convection	Hastelloy N	607	212	14,615	Test continuing
LiF-BeF_2-ThF_4-UF_4 (68-20-11.7-0.3)	Thermal convection	Hastelloy N	704	340	15,930	Test continuing
LiF-BeF_2-ThF_4-UF_4 (68-20-11.7-0.3) plus bismuth in molybdenum hot finger	Thermal convection	Hastelloy N	704	340	4660	Test continuing
$NaBF_4$-NaF (92-8)	Thermal convection	Hastelloy N	687	480	10,515	Test continuing

point is below the critical temperature for steam, that is, 706°F. One of the outstanding advantages of the fluoroborate salt is that its melting point is 725°F, only about 20°F above the critical temperature for water. Flinak, on the other hand, has a melting point of 876°F, 170°F above the critical temperature. The temperature difference is so large for the latter that thermal stress problems under steam-generator startup conditions would be severe in heat exchangers of conventional design. Fortunately, the reentry tube steam generator proposed in a companion report[20] makes use of a steam blanket between the boiling water and the molten salt so that a large temperature difference between the two probably can be accommodated without difficulties with salt freezing, heat transfer instabilities associated with film boiling, or severe thermal stresses. This favorable set of conditions in the steam generator should hold over the whole range of conditions from zero to full power including transients and off-design operating conditions. As a consequence, the difference in melting point is not a controlling consideration in the use of fluoroborate salt rather than Flinak from the steam generator standpoint.

Leakage Problems

ORNL experience with high-temperature liquid systems has shown that, while the probability of small leaks between systems can be kept very low, it is not possible to assure that a small leak will never occur in a heat exchanger. Thus it becomes important to choose the fluids in systems coupled by a heat exchanger so that a small leak from either system into the other will not lead to a rapidly progressing failure or to a mess that cannot be cleaned up readily. For example, in the ANP systems it was found that leakage of NaK into systems containing a fuel-bearing salt or vice versa led to the formation of deposits that are highly insoluble in either water or the molten salts, and hence could not be flushed from the system in which they formed. Fortunately, it appears that either the fluoroborate salt or the Flinak would be compatible with either the fuel salt or the steam in this respect. Contamination of the fuel salt by substantial quantities of either boron or natural lithium would pose problems, the ^{6}Li being much more serious.

Off-Gas Problems

In any practical system it is always necessary to have one or more gas lines coupled to the gas space over the liquid in the expansion tank. A variety of troubles has been experienced with material distilling off into these gas lines, particularly in systems in which the vapor pressure of the salt has been appreciable. The limited experience available to date with 92 $NaBF_4$-8 NaF (which has a vapor pressure of 160 mm at 1125°F) indicates that the problems posed by this material as a consequence of the evolution of BF_3 are manageable, but do require care in the design and operation of the system. The vapor pressure of Flinak is so low that it has never given trouble of this sort.

Heat Transfer Performance

The physical properties of the molten salt used in the intermediate fluid circuit affect not only the size and cost of the intermediate heat exchanger and the boiler, but they also affect the pumping power, the size of the piping, and, as noted above, the fuel inventory. The physical properties of Flinak make it clearly superior to the fluoroborate salt as a heat transfer and heat transport fluid, the difference running from 20 to 25% in favor of Flinak in all of these items.

Tritium Leakage

Tritium generated in Flinak by delayed neutrons released from the fuel in the intermediate heat exchanger would diffuse into the steam system and thus would introduce hazards problems. The problems are essentially similar to those posed by tritium generation in the fuel salt, but it appears that they can be handled more readily if fluoroborate is employed rather than Flinak.

REFERENCES

1. A. P. Fraas, Conceptual Design of a Molten Salt Reactor with Its Intermediate Heat Exchangers and Fuel Pumps Integrated in a Common Pressure Vessel, internal ORNL memorandum, April 13, 1971.

2. M. M. Yarosh, Evaluation of the Performance of Liquid Metal and Molten Salt Heat Exchangers, Nucl. Sci. and Eng., 8: 32 (1960).

3. E. N. Sieder and G. E. Tate, Heat Transfer and Pressure Drop of Liquids in Tubes, Ind. Eng. Chem., 28: 1429–1435 (1936).

4. A. P. Colburn, A Method of Correlating Forced Convection Heat Transfer Data and a Comparison with Fluid Friction, Trans. AIChE, 29: 174–209 (1933).

5. P. Miller, J. J. Byrnes, and D. M. Benforado, Heat Transfer to Water Flowing Parallel to a Rod Bundle, AIChE Jour., 2: 226–235 (1956).

6. B. Lubarsky and S. J. Kaufman, Review of Experimental Investigations of Liquid-Metal Heat Transfer, NACA TR 1270, 1956.

7. A. P. Fraas and M. N. Ozisik, pp. 60–61, Heat Exchanger Design, John Wiley & Sons, New York, 1965.

8. J. R. McWherter, MSBR Mark I Primary and Secondary Salts and Their Physical Properties, internal memorandum MSR 68–135, Sept. 27, 1968.

9. J. H. DeVan and R. B. Evans, III, Corrosion Behavior of Reactor Materials in Fluoride Salt Mixtures, USAEC Report ORNL-TM-328, Oak Ridge National Laboratory, Sept. 19, 1962.

10. J. H. DeVan and R. S. Crouse, Examination of Nickel-Molybdenum Forced Circulation Loop 7641-9, Oak Ridge National Laboratory, unpublished internal document, Aug. 13, 1957.

11. J. H. DeVan and R. S. Crouse, Examination of Hastelloy B Pump Loops 7641-1B and 7641-2B, Oak Ridge National Laboratory, unpublished internal document, Jan. 17, 1957.

12. MSRP Quarterly Progr. Rept. July 31, 1959, USAEC Report ORNL-2799, Oak Ridge National Laboratory.

13. MSRP Quarterly Progr. Rept. Jan. 31, 1959, USAEC Report ORNL-2684, Oak Ridge National Laboratory.

14. MSRP Quarterly Progr. Rept. Oct. 31, 1958, USAEC Report ORNL-2626, Oak Ridge National Laboratory.

15. MSRP Quarterly Progr. Rept. June 30, 1958, USAEC Report ORNL-2551, Oak Ridge National Laboratory.

16. MSRP Quarterly Progr. Rept. Jan. 31, 1958, USAEC Report ORNL-2474, Oak Ridge National Laboratory.

17. J. W. Koger and A. P. Litman, Compatibility of Hastelloy N and Croloy 9M with $NaBF_4$-NaF-KBF_4 (90-4-6 mole %) Fluoroborate Salt, USAEC Report ORNL-TM-2490, April 1969.

18. MSRP Semiann. Progr. Rept. Feb. 29, 1968, pp. 218–225, USAEC Report ORNL-4254, Oak Ridge National Laboratory.

19. MSRP Semiann. Progr. Rept. Aug. 31, 1970, pp. 166–176, USAEC Report ORNL-4622, Oak Ridge National Laboratory.

20. A. P. Fraas, A New Approach to the Design of Steam Generators for Molten Salt Reactor Power Plants, USAEC Report ORNL-TM-2953, Oak Ridge National Laboratory (to be published).

APPENDICES

APPENDIX A

Solution of the Heat Exchanger Equations

This appendix gives details of the elimination process involved in going from the equation set, Eqs. 12 through 22, to the single equation in tube-side mass flow, Eq. 23. We begin by using Eqs. 12 and 22 of the text to eliminate the shell-side flow area from the set, giving

$$G_s N D_s = \frac{C_1}{C_{11}} . \tag{A-1}$$

We next eliminate the shell-side heat transfer coefficient between Eqs. 14 and 17 and the tube-side heat transfer coefficient between Eqs. 15 and 18 to give

$$L^{1-S_2} N D_s^{S_2+S_3-1} G_s^{S_3} \Delta T_s = \frac{C_3}{C_6} , \tag{A-2}$$

$$L^{1-T_2} N D_t^{T_3} \Delta T_t = \frac{C_4}{C_7} . \tag{A-3}$$

By combining Eqs. 16 and 19 with Eqs. A-2 and A-3 the three temperature differences through the two fluid films and the tube wall may be eliminated at one fell swoop to give

$$L^{-1} N^{-1} \left[\frac{C_3}{C_6} G_s^{-S_3} D_s^{1-S_2-S_3} L^{S_2} + C_5 + \frac{C_4}{C_7} G_t^{-T_3} L^{T_2} \right] = C_8 . \tag{A-4}$$

We now obtain an expression for the product LN from Eqs. 13 and 21,

$$L^{-1} N^{-1} = \frac{G_t^{3-T_5}}{C_2 C_{10}} , \tag{A-5}$$

using it in Eq. A-4 to obtain

$$\frac{C_3}{C_2C_6C_{10}}G_t^{3-T_5}G_s^{-S_3}D_s^{1-S_2-S_3}L^{S_2} + \frac{C_5}{C_2C_{10}}G_t^{3-T_5}$$

$$+ \frac{C_4}{C_2C_7C_{10}}G_t^{3-T_3-T_5}L^{T_2} = C_8 \ . \qquad \text{(A-6)}$$

The number of tubes, N, may be eliminated between Eqs. 13 and A-1 to give

$$G_sG_t^{-1}D_s = \frac{C_1}{C_2C_{11}} \ . \qquad \text{(A-7)}$$

A rewriting of Eq. 21 yields an expression for the tube length, L,

$$L = C_{10}G_t^{T_5-2} \ , \qquad \text{(A-8)}$$

which may then be used to eliminate tube length from Eqs. 20 and A-6, giving

$$G_s^{2-S_5}G_t^{T_5-2}D_s^{-1-S_5} = \frac{C_9}{C_{10}} \qquad \text{(A-9)}$$

and

$$\frac{C_3C_{10}^{S_2}}{C_2C_6C_{10}}G_t^{3-T_5+S_2(T_5-2)}G_s^{-S_3}D_s^{1-S_2-S_3} + \frac{C_5}{C_2C_{10}}G_t^{3-T_5}$$

$$+ \frac{C_4C_{10}^{T_2}}{C_2C_7C_{10}}G_t^{3-T_3-T_5+T_2(T_5-2)} = C_8 \ . \qquad \text{(A-10)}$$

From Eq. A-7, we obtain an expression for the shell side equivalent diameter, D_s,

$$D_s = \frac{C_1}{C_2C_{11}}G_tG_s^{-1} \ . \qquad \text{(A-11)}$$

Then, using this expression in Eqs. A-9 and A-10, we obtain Eqs. A-12 and A-13,

$$G_s^3 G_t^{-3-S_5+T_5} = \frac{C_9}{C_{10}}\left[\frac{C_1}{C_2C_{11}}\right]^{1+S_5} \tag{A-12}$$

$$\frac{C_3C_{10}^{S_2}}{C_2C_6C_{10}}\left[\frac{C_1}{C_2C_{11}}\right]^{1-S_2-S_3} G_t^{4-S_3-T_5+S_2(T_5-3)} G_s^{S_2-1} + \frac{C_5}{C_2C_{10}} G_t^{3-T_5}$$

$$+ \frac{C_4C_{10}^{T_2}}{C_2C_7C_{10}} G_t^{3-T_3-T_5+T_2(T_5-2)} = C_8 \ , \tag{A-13}$$

in which the only remaining unknowns are the two mass flows, G_s and G_t. Finally, we eliminate the shell-side flow from Eq. A-13 by using

$$G_s = \left[\frac{C_9}{C_{10}}\left(\frac{C_1}{C_2C_{11}}\right)^{1+S_5}\right]^{1/3} G_t^{1+(S_5-T_5)/3} \ , \tag{A-14}$$

which is simply a rearrangement of Eq. A-12, to give a single equation in which the only unknown is the tube-side mass flow, G_t.

$$G_t^{3-T_5} +$$

$$\frac{C_3C_{10}^{S_2}}{C_5C_6}\left[\frac{C_9}{C_{10}}\right]^{(S_2-1)/3}\left[\frac{C_1}{C_2C_{11}}\right]^{1-S_2-S_3+(S_2-1)(1+S_5)/3} G_t^{3-2S_2-S_3+(S_2-1)(2T_5+S_5)/3}$$

$$+ \frac{C_4C_{10}^{T_2}}{C_5C_7} G_t^{3-T_3-T_5+T_2(T_5-2)} - \frac{C_2C_8C_{10}}{C_5} = 0 \ . \tag{A-15}$$

Now, defining coefficients C_{19}, C_{20}, and C_{21} by

$$C_{19} = \frac{C_2C_8C_{10}}{C_5} \ , \tag{A-16}$$

$$C_{20} = \frac{C_3C_{10}^{S_2}}{C_5C_6}\left[\frac{C_9}{C_{10}}\right]^{(S_2-1)/3}\left[\frac{C_1}{C_2C_{11}}\right]^{1-S_2-S_3+(S_2-1)(1+S_5)/3} \ , \tag{A-17}$$

$$C_{21} = \frac{C_4 C_{10}^{T_2}}{C_5 C_7} , \qquad \text{(A-18)}$$

and exponents E_1, E_2, and E_3 by

$$E_1 = 3-T_5 , \qquad \text{(A-19)}$$

$$E_2 = 3-2S_2-S_3+(S_2-1)(2T_5+S_5)/3 , \qquad \text{(A-20)}$$

$$E_3 = 3-T_3-T_5+T_2(T_5-2) , \qquad \text{(A-21)}$$

we reduce Eq. A-15 to

$$G_t^{E_1} + C_{20} G_t^{E_2} + C_{21} G_t^{E_3} - C_{19}^{\wedge} = 0 , \qquad \text{(23)}$$

which is Eq. 23 of the text.

APPENDIX B. FORTRAN PROGRAM FOR COMPUTER SOLUTION OF THE HEAT EXCHANGER EQUATIONS

A brief description of the operation of a FORTRAN program written for solving the heat exchanger equations presented in this report is given in this Appendix. A computer-prepared printout of the program follows the description. Instructions for program use will be found in Appendix C.

Program Line No.	Operation
1 – 3	Program identification.
100 – 110	Declaration statements.
115 – 125	Compute various constants needed later in the program.
130 – 135	Advance case number; note that this yields an initial case number equal to one, if not specified. Read and test "NIN"; stop if zero or negative.
140	Read NIN values into locations J in array DAT.
145 – 185	Set program variables from array; print case number.
190 – 215	Convert units; compute quantities needed later.
220 – 335	Compute coefficients C_1 through C_{21} and exponents E_1 through E_5. Assume turbulent flow, both fluids. Compute estimate for G_t from Eq. 24.
340 – 370	Newton's Method iteration for G_t; if converged, to line 380.
375	If iteration fails to converge in 10 trials, print warning message and continue.
380 – 430	Compute G_s corresponding to G_t; compute actual flow regime and compare with assumed. If in agreement, to line 460; otherwise, to appropriate line, 435–450.
435	Assume laminar flow on tube side. Repeat 280–430.
440	Assume laminar flow on shell side. Repeat 280–430.
445	Assume turbulent flow, tube side. Repeat 280–430.
450 – 455	Arrival here means that no combination of assumed flows yields a self-consistent result. Program gives up, prints warning message, and reads in the data for the next case. (This has never happened in any of the many calculations made to date.)
460 – 650	Compute remaining dependent variables, edit, and print.
655	Return to read in data for next case.

660	Program stop.
665 – 700	Subroutines for setting coefficients and exponents according to flow regime. See Table 3.
705	Input data bank stored after this line.

HEATX2

```
1*      HEATX2.  HEAT EXCHANGER DESIGN.  M. LAVERNE. 9102 3-5702
2*      19 MAR 1970
3*
100    REAL MUS, MUT, KS, KT, KWALL, LTUBE, NTUBE
105    DIMENSION DAT(20)
110    COMMON CLAM,CURT,S1,S2,S3,S4,S5,T1,T2,T3,T4,T5
115    PI = 3.141592654; PI04 = PI/4.
120    CURT = 1./3.; CLAM = 4./10.↑CURT
125    TWOGC = 64.348*3600.↑2; COO = .5*PI/SQRT(3.)
130 1  DAT(20) = DAT(20)+1.0
135    READ, NIN; IF(NIN) 21,21
140    READ,(J,DAT(J),I=1,NIN)
145    Q = DAT(1)
150    DPS = DAT(2); TSI = DAT(3); TSO = DAT(4)
155    CPS = DAT(5); MUS = DAT(6);  KS = DAT(7); RHOS = DAT(8)
160    DPT = DAT(9); TTI = DAT(10); TTO = DAT(11)
165    CPT = DAT(12); MUT = DAT(13); KT = DAT(14); RHOT = DAT(15)
170    DO = DAT(16); TW = DAT(17); KWALL = DAT(18)
175    RHOW = DAT(19); ICASE = DAT(20)
180    PRINT 30, ICASE
185 30FORMAT(/"CASE ", I3)
190    DPS = 144.*DPS; DPT = 144.*DPT
195    DO = DO/12.; TW = TW/12.; DT = DO-2.*TW
200    AO = PI04*DO*DO; AT = PI04*DT*DT; AW = AO-AT
205    DTS = TSI-TSO; DTT = TTO-TTI
210    DT1 = TSI-TTO; DT2 = TSO-TTI
215    DM = (DO-DT)/LOG(DO/DT)
220    CO8 = DT1; IF(DT1-DT2) 2,3,2
225 2  CO8 = (DT1-DT2)/LOG(DT1/DT2)
230 3  CO5 = Q/PI
235    CO1 = Q/(CPS*DTS); CO2 = Q/(AT*CPT*DTT)
240    CO3 = CO5/DO; CO4 = CO5/DT; CO5 = CO5*TW/(DM*KWALL)
245    CO6A = (CPS*KS↑2*MUS)↑CURT
250    CO7A = (CPT*KT↑2*MUT)↑CURT/DT
255    CO9A = TWOGC*RHOS*DPS
260    C10A = TWOGC*RHOT*DPT*DT
265    C11 = PI04*DO; C12 = CO1/(CO2*C11); C13 = CO3/CO5
270    C14 = CO4/CO5; C15 = CO2*CO8/CO5; N = 0
275    CALL STURB; CALL TTURB; IAS = IAT = 1
280 4  CO6 = CO6A*S1/MUS↑S3
285    CO7 = CO7A*T1*DT↑(T2+T3)/MUT↑T3
290    CO9 = CO9A/(S4*MUS↑S5)
295    C10 = C10A*(DT/MUT)↑T5/T4
300    C16 = C13/CO6; C17 = CO9/C10; C18 = C14/CO7
305    C19 = C15*C10
310    E1 = 3.-T5; E4 = (S2-1.)/3.
315    E2 = 3.-2.*S2-S3+E4*(2.*T5+S5)
320    E3 = E1-T3+T2*(T5-2.)
325    E5 = 1.-S2-S3+E4*(1.+S5)
330    C20 = C16*C10↑S2*C17↑E4*C12↑E5
```

HEATX2 CONTINUED

```
335    C21 = C18*C10↑T2; GT = 0.9*(C19/(C20+C21))↑(1./E2)
340    DO 5 I = 1, 10
345    GT1 = GT↑E1; GT2 = GT↑E2; GT3 = GT↑E3
350    GT20 = C20*GT2; GT21 = C21*GT3
355    FUN = GT1+GT20+GT21-C19
360    DER = (E1*GT1+E2*GT20+E3*GT21)/GT; DGT = FUN/DER
365    GT = GT-DGT; IF(ABS(DGT/GT)-1.E-5) 6
370 5  CONTINUE
375    PRINT, ↑↑"NOT CONVERGED.  DGT/GT =", DGT/GT
380 6  GSOGT = (C17*C12↑(1.+S5)*GT↑(S5-T5))↑CURT
385    GS = GT*GSOGT; DS = C12/GSOGT
390    RET = GT*DT/MUT; RES = GS*DS/MUS
395    ICT = 0; IF(RET-1502.) 7; ICT = 1
400 7  NT = 0; IF(IAT-ICT) 9,8,9
405 8  NT = 1
410 9  ICS = 0; IF(RES-994.) 10; ICS = 1
415 10NS = 0; IF(IAS-ICS) 12,11,12
420 11NS = 1
425 12IF(NT*NS) 13,13,18
430 13N = N+1; GO TO (14,15,16,17) N
435 14CALL TLAM ; IAT = 0; GO TO 4
440 15CALL SLAM ; IAS = 0; GO TO 4
445 16CALL TTURB; IAT = 1; GO TO 4
450 17PRINT, "ASSUMED AND CALCULATED REGIMES DO NOT AGREE."
455    GO TO 1
460 18LTUBE = C10*GT↑(T5-2.); NTUBE = C02/GT
465    AS = C01/GS; HS = C06*(DS*GS)↑S3*(DS/LTUBE)↑S2/DS
470    VS = GS/RHOS; VT = GT/RHOT
475    HPS = DPS*AS*VS/1.98E6; HPT = DPT*AT*NTUBE*VT/1.98E6
480    HT = C07*GT↑T3/LTUBE↑T2; DTW = C05/(LTUBE*NTUBE)
485    FDTT = C14*DTW/HT; FDTS = C13*DTW/HS
490    S = SQRT(C00*DO*(DS+DO))
495    BUNWT = LTUBE*(NTUBE*(AT*RHOT+AW*RHOW)+AS*RHOS)
500    PRINT 20,0,12.*DO,12.*TW,12.*DT,KWALL,RHOW
505    PRINT 22,DPS/144.,TSI,TSO,CPS,MUS,KS,RHOS,
510   +DPT/144.,TTI,TTO,CPT,MUT,KT,RHOT
515    PRINT 24, NTUBE,LTUBE,12.*S,12.*DS,
520   +AS*LTUBE,AT*LTUBE*NTUBE,AW*LTUBE*NTUBE,BUNWT
525    PRINT 26,C08,DTW,FDTS,HS,FDTT,HT
530    PRINT 28,GT/GS,GS,VS/3600.,HPS,RES,GT,VT/3600.,HPT,RET
535
540 20FORMAT(/3X"HEAT"3X4(4X"TUBE")7X"TUBE"/
545   +3X"LOAD"7X"O.D."4X"WALL"4X"I.D."6X"K"7X"DENSITY"/
550   +2X"BTU/HR "3(6X"IN")2X"BTU/HR FT F  LB/FT↑3"/
555   +1PE10.3,0P3F8.4,F9.2,F11.1)
560
565 22FORMAT(//7X"P DROP  T IN   T OUT  SP. HEAT  VISCOS'Y
570   +  CONDUCTIV'Y  DENSITY"/9X"PSI"5X"F"6X"F"4X"BTU/LB F
575   +  LB/HR FT  BTU/HR FT F  LB/FT↑3"/
580   +" FUEL:"F6.0,F8.0,F7.0,F8.3,F10.2,F11.2,F12.1/
```

HEATX2 CONTINUED

```
585   +" SALT:"F6.0,F8.0,F7.0,F8.3,F10.2,F11.2,F12.1)
590
595 24FORMAT(//" NUMBER"4X2("TUBE"4X)"EQUIV."6X"VOLUMES"7X"BUNDLE"/
600   +"OF TUBES  LENGTH  SPACING  DIAM'R  FUEL  SALT  TUBE"2X"WEIGHT"/
605   +12X"FT "2(5X"IN"2X)3(2X"FT↑3")4X"LB"/F7.0,F8.1,2F9.4,3F6.1,F8.0)
610
615 26FORMAT(//4X"LMTD  WALL DT"10X"FILM DT  COEFFICIENT"/
620   +5X"F"7X"F"16X"F"4X"BTU/HR FT↑2 F"/2F8.1,3X" FUEL:",
625   +F8.1,F11.0/20X"SALT:",F8.1,F11.0)
630
635 28FORMAT(//"FLOW RATIO"11X"FLOWS"4X"VELOCITIES  PUMPING
640   +  REYNOLDS"/3X"GT/GS"11X"LB/HR FT↑2   FT/SEC"6X"HP"
645   +5X"NUMBERS"/F8.4,4X" FUEL:"1PE11.4,0PF8.1,F11.0,F10.0/
650   +13X"SALT:"1PE11.4,0PF8.1,F11.0,F10.0//)
655    GO TO 1
660 21STOP
665    SUBROUTINE SLAM; COMMON CLAM,CURT,S1,S2,S3,S4,S5,T1,T2,T3,T4,T5
670    S1=CLAM; S2=S3=CURT; S4=64.; S5=1.; RETURN
675    SUBROUTINE TLAM; COMMON CLAM,CURT,S1,S2,S3,S4,S5,T1,T2,T3,T4,T5
680    T1=CLAM; T2=T3=CURT; T4=64.; T5=1.; RETURN
685    SUBROUTINE STURB;COMMON CLAM,CURT,S1,S2,S3,S4,S5,T1,T2,T3,T4,T5
690    S1=.032; S2=0.; S3=.8; S4=.256; S5=.2; RETURN
695    SUBROUTINE TTURB;COMMON CLAM,CURT,S1,S2,S3,S4,S5,T1,T2,T3,T4,T5
700    T1=.023; T2=0.; T3=.8; T4=.184; T5=.2; RETURN
705    $DATA
```

```
LENGTH
ABOUT 5800 CHARS.
```

APPENDIX C

SAMPLE COMPUTER PROGRAM INPUT AND OUTPUT

This Appendix contains information on the preparation of input for the computer program described in Appendix B. A suggested input form, completed, and the corresponding paper tape information are shown, followed by a sample printout from a computer run.

Table C-1 shows a suggested input form for HEATX2, with data entered for two sample cases. Note that the given units are not completely consistent but are specified for convenience. Conversion to a consistent set is performed internally by the program.

For each item specified in the column headed "DAT(I)", the corresponding "I" must be given. Also, the pairs of input numbers specified must agree with the corresponding number at the top of the form. Note that for the first case a complete set of input (the first 19 items) must be given. The initial case number need not be specified, in which case the program will start with "one", incrementing by unity for each succeeding case.

For all cases after the first, only those items differing from the immediately preceding case need be changed. Note that if item 20, "Case Number", is specified, the normal sequence of consecutive case numbers is interrupted, continuing with the new value.

A normal termination of the computer run is obtained by specifying "NIN", the pairs of input numbers, to be zero or negative. If "NIN" is omitted, inadvertently or otherwise, an abnormal termination will occur, with an error message that may be disregarded.

Table C-2 is a printout of a paper tape prepared from the specifications of Table C-1. The line numbers shown are not essential; the existing program ends at line 705, so that any greater line number will suffice for starting the tape. It is suggested that an initial line number of roughly 800 or greater be used for input to allow for possible program expansion.

The input is free-form, i.e., the numbers may be typed in any convenient form (note the mixture of exponential, fixed-point, and integer forms) with as many or as few numbers per line as convenient. It may be

Pairs of Input Numbers		19		5		0	
Quantity	Units	I	DAT(I)	I	DAT(I)	I	DAT(I)
Heat Load	Btu/hr	1	1.25E9				
Shell Side: Pressure Drop	Psi	2	100				
Inlet Temperature	^{o}F	3	1300				
Outlet Temperature	^{o}F	4	1050				
Fluid Specific Heat	Btu/lb ^{o}F	5	.324				
" Viscosity	Lb/hr ft	6	23.5				
" Conductivity	Btu/hr ft ^{o}F	7	.58				
" Density	Lb/ft^3	8	208				
Tube Side: Pressure Drop	Psi	9	100				
Inlet Temperature	^{o}F	10	950				
Outlet Temperature	^{o}F	11	1200				
Fluid Specific Heat	Btu/lb ^{o}F	12	.36	12	.437		
" Viscosity	Lb/hr ft	13	1.95	13	12.6		
" Conductivity	Btu/hr ft ^{o}F	14	.266	14	2.66		
" Density	Lb/ft^3	15	119	15	132		
Tubes: O. D.	In	16	.3125				
Wall Thickness	In	17	.023				
" Conductivity	Btu/hr ft ^{o}F	18	11.5				
" Density	Lb/ft^3	19	531				
Case Number	- - -			20	19		

Table C-1. Input Form for HEATX2, Showing Sample Input for Two Cases.

```
800    19
801    1.25E9
802    2 100 3 1300 4 1050 5 .324 6 23.5 7 .58 8 208
803    9 100 10 950 11 1200 12 .36 13 1.95 14 .266 15 119
804    16 .3125 17 .023 18 11.5 19 531
805    5
806    12 .437 13 12.6 14 2.66 15 132
807    20 19
808    0
```

Table C-2. Printout of Paper Tape Prepared from Data of Table C-1.

seen by comparing Tables C-1 and C-2 that the particular grouping used puts similar items on one line.

The results of a computer run, using the input tape of Table C-2, are shown in Table C-3. The program spaces the printouts to give two cases per page.

CASE 1

HEAT LØAD BTU/HR	TUBE Ø.D. IN	TUBE WALL IN	TUBE I.D. IN	TUBE K BTU/HR FT F	TUBE DENSITY LB/FT↑3
1.252E+09	.3125	.0230	.2665	11.50	531.0

	P DRØP PSI	T IN F	T ØUT F	SP. HEAT BTU/LB F	VISCØS'Y LB/HR FT	CØNDUCTIV'Y BTU/HR FT F	DENSITY LB/FT↑3
FUEL:	100.	1300.	1050.	.324	23.50	.58	208.0
SALT:	100.	950.	1200.	.360	1.95	.27	119.0

NUMBER ØF TUBES	TUBE LENGTH FT	TUBE SPACING IN	EQUIV. DIAM'R IN	VØLUMES FUEL FT↑3	SALT FT↑3	TUBE FT↑3	BUNDLE WEIGHT LB
4944.	31.5	.4106	.2823	74.9	60.3	22.6	34757.

LMTD F	WALL DT F		FILM DT F	CØEFFICIENT BTU/HR FT↑2 F
100.0	17.7	FUEL:	47.0	2091.
		SALT:	35.2	3271.

FLØW RATIØ GT/GS		FLØWS LB/HR FT↑2	VELØCITIES FT/SEC	PUMPING HP	REYNØLDS NUMBERS
1.1179	FUEL:	6.4973E+06	8.7	540.	6504.
	SALT:	7.2632E+06	17.0	850.	82720.

CASE 19

HEAT LØAD BTU/HR	TUBE Ø.D. IN	TUBE WALL IN	TUBE I.D. IN	TUBE K BTU/HR FT F	TUBE DENSITY LB/FT↑3
1.252E+09	.3125	.0230	.2665	11.50	531.0

	P DRØP PSI	T IN F	T ØUT F	SP. HEAT BTU/LB F	VISCØS'Y LB/HR FT	CØNDUCTIV'Y BTU/HR FT F	DENSITY LB/FT↑3
FUEL:	100.	1300.	1050.	.324	23.50	.58	208.0
SALT:	100.	950.	1200.	.437	12.60	2.66	132.0

NUMBER ØF TUBES	TUBE LENGTH FT	TUBE SPACING IN	EQUIV. DIAM'R IN	VØLUMES FUEL FT↑3	SALT FT↑3	TUBE FT↑3	BUNDLE WEIGHT LB
4444.	28.1	.4132	.2899	61.7	48.4	18.2	28871.

LMTD F	WALL DT F		FILM DT F	CØEFFICIENT BTU/HR FT↑2 F
100.0	22.1	FUEL:	55.2	2218.
		SALT:	22.7	6324.

FLØW RATIØ GT/GS		FLØWS LB/HR FT↑2	VELØCITIES FT/SEC	PUMPING HP	REYNØLDS NUMBERS
.9456	FUEL:	7.0404E+06	9.4	540.	7237.
	SALT:	6.6575E+06	14.0	631.	11734.

Table C-3. Computer Printout of Results for Input Data of Table C-1.

INTERNAL DISTRIBUTION

1. J. L. Anderson
2. H. F. Bauman
3. S. E. Beall
4. M. Bender
5. C. E. Bettis
6. E. S. Bettis
7. E. G. Bohlmann
8. C. J. Borkowski
9. H. I. Bowers
10. R. B. Briggs
11. C. W. Collins
12. J. W. Cooke
13. W. B. Cottrell
14-16. J. L. Crowley
17. F. L. Culler
18. J. R. DiStefano
19. S. J. Ditto
20. W. P. Eatherly
21. J. R. Engel
22. D. E. Ferguson
23-32. A. P. Fraas
33. L. D. Fuller
34. W. R. Grimes
35. A. G. Grindell
36. W. O. Harms
37. P. N. Haubenreich
38. R. E. Helms
39. H. W. Hoffman
40. P. R. Kasten
41. J. J. Keyes, Jr.
42. M. E. LaVerne
43. M. I. Lundin
44. R. N. Lyon
45. H. G. MacPherson
46. R. E. MacPherson
47. H. E. McCoy
48. H. C. McCurdy
49. H. A. McLain
50. L. E. McNeese
51. J. R. McWherter
52. A. J. Miller
53. R. L. Moore
54. E. L. Nicholson
55. A. M. Perry
56. R. C. Robertson
57-66. M. W. Rosenthal
67. J. P. Sanders
68. A. W. Savolainen
69-70. Dunlap Scott
71. M. J. Skinner
72. I. Spiewak
73. D. A. Sundberg
74. R. E. Thoma
75. D. B. Trauger
76. A. M. Weinberg
77. J. R. Weir
78. M. E. Whatley
79. G. D. Whitman
80. L. V. Wilson
81-82. Central Research Library
83. Document Reference Section
84-86. Laboratory Records
87. Laboratory Records (LRD-RC)

EXTERNAL DISTRIBUTION

88. David Elias, AEC, Washington
89. R. Jones, AEC, Washington
90. Kermit Laughon, AEC-OSR
91-92. T. W. McIntosh, AEC, Washington
93. M. Shaw, AEC, Washington
94. W. L. Smalley, AEC-ORO
95-96. Division of Technical Information Extension (DTIE)
97. Laboratory and University Division, ORO
98-99. Director, Division of Reactor Licensing, AEC, Washington
100-101. Director, Division of Reactor Standards, AEC, Washington
102-106. Executive Secretary, Advisory Committee on Reactor Safeguards